The Systematized Collection of Daubechies Wavelets

Carl Taswell
UCSD School of Medicine, La Jolla, CA 92093-0603
Computational Toolsmiths, Stanford, CA 94309-9925

Abstract

A single unifying algorithm has been developed to systematize the collection of compact Daubechies wavelets. This collection comprises all classes of real and complex orthogonal and biorthogonal wavelets with the maximal number K of vanishing moments for their finite length. Named and indexed families of wavelet filters were generated by spectral factorization of a product filter in which the optimal subset of roots was selected by a defining criterion within a combinatorial search of subsets meeting required constraints. Several new families have been defined some of which were demonstrated to be equivalent to families with roots selected solely by geometric criteria that do not require an optimizing search. Extensive experimental results are tabulated for $1 \leq K \leq 24$ for each of the families and most of the filter characteristics defined in both time and frequency domains. For those families requiring optimization, a conjecture for $K > 24$ is provided for a search pattern that reduces the order of the computational complexity but permits attainment of the desired optimum.

Technical Report CT-1998-06: original 5/22/98; revision 6/23/98.
Carl Taswell, Computational Toolsmiths, Stanford, CA 94309-9925
Email: taswell@toolsmiths.com; Tel: 650-323-4336, Fax: 650-323-5779

0 List of Symbols

$\mathcal{D}$, $\mathcal{L}$ in upper case calligraphic font for Daubechies parameter and Lagrange parameter;

N, M, K, R in upper case math font for filter bank related parameters;

d, p in lower case math font for degree and parity or power parameters;

n, t, z in lower case math font for independent variables in discrete time, continous time, and complex z-domain;

$z = re^{i\alpha}$ for complex z with radius r, imaginary i, angle α;

α, ω in lower case Greek font for angle and frequency in radians;

$\mathcal{P}$, $\mathcal{A}$, $\mathcal{S}$, $\mathcal{F}$, $\mathcal{G}$, $\mathcal{H}$ in upper case calligraphic font for polynomials (usually expressed as $\mathcal{P}(z)$ in terms of roots z);

$\mathbf{p}$, $\mathbf{a}$, $\mathbf{s}$, $\mathbf{f}$, $\mathbf{g}$, $\mathbf{h}$ in lower case bold font for vectors of coefficients;

$\mathbf{A}$, $\mathbf{S}$, $\mathbf{F}$, $\mathbf{G}$, $\mathbf{H}$ in upper case bold font for matrices of coefficients;

i, j, k, m, n in lower case math font for running indices in sums or products, or for subscript indices in vectors or matrices;

n^{cq}, n^{rd} with number n in lower case math font and superscripts in roman font;

N_p, N_a, N_s, n_p^{cq}, n_a^{cq}, n_s^{cq} various numbers with subscripts p, a, and s for product, analysis, and synthesis filters;

γ, η, ϕ, ψ, τ, ε, φ, ρ in lower case Greek fonts for gamma, eta, phi, psi, tau, varepsilon, varphi, rho;

$\boldsymbol{\varsigma}$, $\boldsymbol{\upsilon}$, $\boldsymbol{\nu}$, $\boldsymbol{\varepsilon}$ in lower case Greek bold font for varsigma, upsilon, nu, varepsilon;

Φ, Ψ, Υ in upper case Greek fonts for Phi, Psi, Upsilon;

Contents

0 List of Symbols **3**

1 Introduction **5**

2 Methods **7**

2.1 Computation of Filter Roots . . . 7
2.1.1 Symmetric Positive Laurent Polynomials . . . 7
2.1.2 Lagrange Polynomials . . . 8
2.1.3 Daubechies Polynomials . . . 10
2.2 Generation of Filter Coefficients . . . 11
2.2.1 Discrete Impulse Response . . . 11
2.2.2 Continuous Impulse Response . . . 12
2.2.3 Reconstructing Filter Banks . . . 13
2.3 Evaluation of Filter Parameters . . . 15
2.3.1 Coefficient and Root Errors . . . 15
2.3.2 M^{th}-Band Interpolation Error . . . 16
2.3.3 Phase NonLinearity . . . 16
2.3.4 Other Filter Parameters . . . 17
2.4 Selection of Spectral Factors . . . 18
2.4.1 Factorization Rules . . . 18
2.4.2 Selection Criteria . . . 20
2.4.3 Unifying Algorithm . . . 21
2.5 Hardware and Software . . . 22

3 Results **22**

3.1 Computation of Filter Roots . . . 22
3.2 Generation of Filter Coefficients . . . 24
3.3 Evaluation of Filter Parameters . . . 24
3.4 Selection of Spectral Factors . . . 25
3.5 Comparison of Filter Families . . . 25

4 Discussion **26**

List of Tables

1 List of Named Filters . . . 33
2 Summary of Filter Designs . . . 34
3 Biorthogonal Scalets $\text{tdr}(\mathcal{A})$ and $\text{tdr}(\mathcal{S})$. . . . 35
4 Orthogonal Scalets $\text{tdr}(\mathcal{A})$. . . . 36

5 Biorthogonal Scalets tfu($\mathbf{a}_0$) and tfu($\mathbf{s}_0$). 37
6 Orthogonal Scalets tfu($\mathbf{a}_0$). 38
7 Biorthogonal Scalets fds($\mathbf{a}_0$) and fds($\mathbf{s}_0$). 39
8 Orthogonal Scalets pnl($\mathcal{A}$). 40
9 Biorthogonal Wavelets vmn($\mathbf{a}_1$) and vmn($\mathbf{s}_1$). 41
10 Orthogonal Wavelets vmn($\mathbf{a}_1$). 42

List of Figures

1 Related Forms of Daubechies Polynomial $\mathcal{P}_{\mathcal{D}}(z)$ for $\mathcal{D} = 30$. 43
2 DRNSI(123;62;61) Filter Roots, Impulse Response, Frequency Response. 43
3 LRNSI(323;162;161) Filter Roots, Impulse Response, Frequency Response. 44
4 DRNSI(323;162;161) Filter Roots, Impulse Response, Frequency Response. 44
5 Lagrange and Daubechies Polynomial Root Errors. 45
6 DROMD(4;2) Scalet, QMF, CQF Wavelets with Alternate Parities. 45
7 DCOLA(12;6) Phase NonLinearity. 46
8 DCOMA(12;6) Phase NonLinearity. 46
9 DCOLA(12;6) Spectral Factorization. 47
10 DRBMS(17,15;8,8) Spectral Factorization. 47
11 Daubechies Real Orthogonal Examples. 48
12 Daubechies Complex Orthogonal Examples. 48
13 DCOLN Analysis Scalets. 49
14 DCOLN Analysis Wavelets. 49
15 Phase NonLinearity of Orthogonal Filters. 50
16 Frequency-Domain Selectivity of Biorthogonal Filters. 50

1 Introduction

Numerous discussions of both the general theory [19, 40] and specific parameterizations [29, 54, 53, 22, 34, 38] for Daubechies wavelets have been published since her seminal discovery of compact orthogonal and biorthogonal wavelets [5, 4, 7]. These wavelets, which have the maximal number of vanishing moments for their minimal finite length, can be implemented as discrete filters that are iterated or auto-convolved to generate approximations of the continuous functions. Prior to development of the angular parameterization methods, the Daubechies wavelets were originally designed by spectral factorization of a polynomial (as summarized in her book [6]). This approach has been criticized [54, 38] for the numerical instabilities associated with finding the roots of a polynomial. Yet the angular parameterization methods have not demonstrated any results for much higher order wavelets where the numerical instabilities of the spectral factorization methods begin to occur.

As discussed by Taswell in [47], the advantages and disadvantages of the various approaches should be recognized. The practical utility of each method should be evaluated in terms of the class of wavelet filters and range of filter lengths N for which the method is valid, the possible combinations of desired filter characteristics for which a search can be performed through the method's parameterized space, and the computational complexity of that search for the desired filter. In pursuit of this goal, this article reports a comprehensive evaluation for all classes of Daubechies wavelets, including both real and complex and both orthogonal and biorthogonal, that are computable by spectral factorization.

Both Shensa [37] and Ansari *et al.* [3] related Daubechies filters to Lagrange filters, while Akansu *et al.* [2] related them to binomial filters. Shen and Strang [36] discussed the computation of the Daubechies filter roots as the roots of a binomial polynomial, while Goodman *et al.* [15] considered them as the roots of a Laurent polynomial. More recently, Temme [51] described the asymptotics of the roots in terms of a representation of the incomplete beta function. Other authors have presented Daubechies wavelets generated by complex filters [20, 23] or by real filters optimized for a particular criterion [9, 10, 27, 26, 11].

However, a systematic treatment collecting and evaluating all of the Daubechies real and complex orthogonal and biorthogonal wavelets constructed with a single unifying computational algorithm has not yet appeared in the literature. Such an effort was begun by Taswell [45] focusing on wavelets with varying degrees of asymmetry or symmetry that can be derived by spectral factorization of the Daubechies polynomial. Significant advantages of the spectral factorization approach include its generalizability to many different classes and types of wavelets, its suitability for easily interpretable visual displays, and thus its practicality in pedagogy.

Compact asymmetric and symmetric wavelets include the original orthogonal "extremal phase" and "least asymmetric" families as well as the biorthogonal "spline" and "spline variations" families described by Daubechies [5, 4, 7, 6]. As introduced in the brief report [45], these real families can be extended and systematized to include complex families with a single generalized flexible yet automated algorithm that permits consistent selection of alternative choices and the identification of filters with optimized parameters. As further developed in a subsequent report [50], these parameters now include phase nonlinearity, time-domain regularity, frequency-domain selectivity, and time-frequency uncertainty, but can be readily extended to include other parameters as optimization criteria.

Table 1 lists the named filters in the systematized collection of Daubechies wavelets reported here. For the purposes of this collection, a Daubechies wavelet is considered any orthogonal spectral factor with maximal number of vanishing moments for minimal number of filter coefficients, and any pair of biorthogonal spectral factors such that the sum of the numbers of vanishing moments and filter coefficients for the pair of factors is maximal and minimal, respectively. In essence, the systematized collection comprises all possible spectral factors obtained from either the Lagrange or Daubechies polynomials.

Analytically, both of these polynomials should yield the same roots for spectral factorization. However, numerically with conventional root-finding algorithms, their performance differs signifi-

cantly at higher orders with the Daubechies polynomial outperforming the Lagrange polynomial (Section 3.1). The main collection includes families of lowpass scalet filters as the spectral factors of the product filters. The highpass wavelet filters are then computed from the scalet filters. Sequences of filters derived from spectral factors of products of increasing order include real and complex, orthogonal and biorthogonal, least and most asymmetric, least and most symmetric, symmetric, spline, least uncertain, most selective, most regular, and balanced regular families.

In all but certain cases that do not require an optimization, a combinatorial search algorithm incorporating a binomial subset selection [43, 45] is used to choose the spectral factors (Section 2.4) satisfying the required objective criterion defined for each family. Families have been named according to the defining criterion and indexed according to the number K of zeros at $z = -1$. An explicit composite conformal mapping incorporating an affine transformation and an inverse Joukowski transformation is used to compute the polynomial roots for the spectral factors (Section 2.1.3). Computational algorithms for the generation of the filter coefficients (Section 2.2) and evaluation of the filter parameters (Section 2.3) are presented together with detailed examples demonstrating the methods.

In the filter design process, numerical estimates of filter parameters computed from either filter roots or filter coefficients are used as selection criteria in the search for the spectral factors. However, all empirical filter parameters are evaluated for each optimized filter to determine its performance on criteria other than the selection criterion. Various numerical properties evaluated experimentally for the filters and associated filter banks include those described in the methods [44, 49, 48] for specification, evaluation, and reproducibility of wavelet transform algorithms. Section 3 presents results comparing the various filter families. Section 4 provides a conjecture regarding searches for optimized Daubechies wavelets of higher order K than the range of $1 \leq K \leq 24$ reported in Tables 3–10.

2 Methods

2.1 Computation of Filter Roots

2.1.1 Symmetric Positive Laurent Polynomials

Filter roots for Daubechies scalets and wavelets can be computed by spectral factorization of product filters $\mathcal{P}(z)$ taken to be either the Lagrange polynomials (2.1.2) or the Daubechies polynomials (2.1.3), denoted $\mathcal{P}_{\mathcal{L}}(z)$ and $\mathcal{P}_{\mathcal{D}}(z)$ respectively, as different representations (with distinct parameterizations and computational algorithms) for the same symmetric positive Laurent polynomials. When used as product polynomials in spectral factorization, they can be factored into either orthogonal "square root" factors or other biorthogonal analysis and synthesis factors. When using parameters $\mathcal{D}$ for $\mathcal{P}_{\mathcal{D}}(z)$ and $\mathcal{L} = \mathcal{D} + 1$ for $\mathcal{P}_{\mathcal{L}}(z)$, finding the zeros of these polynomials should analytically yield the same sets of roots. However, results will differ numerically because of the different computational algorithms. As suggested by the author's own unpublished experiments and as confirmed by the comprehensive experiments of Goodman *et al.* [15], computing the eigenvalues

of the companion matrix provides the best performing conventional method[1] for finding the zeros of the Laurent polynomials considered here. Press *et al.* [30, pg 375] provide a concise summary of the companion matrix eigenvalue method for finding zeros of polynomials.

When used for spectral factorization, the product filter polynomials can be factored into

$$\mathcal{P}(z) = \mathcal{A}(z)\mathcal{S}(z) \tag{1}$$

with analysis $\mathcal{A}(z)$ and synthesis $\mathcal{S}(z)$ filter polynomials. In order to be used in the design of orthogonal perfect reconstructing filter banks (PRFB), the product filters $\mathcal{P}(z)$ must satisfy

$$\mathcal{P}(z) = \mathcal{A}(z)\mathcal{A}(z^{-1}) \tag{2}$$

as autocorrelation filters, and

$$\mathcal{P}(z) + \mathcal{P}(-z) = 2 \tag{3}$$

as halfband filters.

Converting from z notation to ω notation, express $z = re^{i\omega}$ with magnitude $r = |z|$ and angle $\omega \in (-\pi, \pi]$. Let $\mathcal{P}(\omega)$ denote $\mathcal{P}(z)$ restricted to the unit circle $r = 1$. Then $\mathcal{P}(z)$ is a halfband autocorrelation filter positive on the unit circle if

$$\mathcal{P}(\omega) = |\mathcal{A}(\omega)|^2 \geq 0 \tag{4}$$

and $\mathcal{A}(\omega)$ is an orthogonal filter if

$$|\mathcal{A}(\omega)|^2 + |\mathcal{A}(\omega + \pi)|^2 = 2. \tag{5}$$

The Féjer-Riesz Theorem ([28, pg 231] or [35, pg 117]) guarantees the existence of the "square root" factor $\mathcal{A}(\omega)$ for positive $\mathcal{P}(\omega)$ a trigonometric polynomial.

2.1.2 Lagrange Polynomials

Lagrange polynomials $\mathcal{P}_{\mathcal{L}}$ can be used in iterative subdivision schemes to perform exact interpolation [8, 37, 3, 16]. They satisfy the autocorrelation and halfband conditions. Express a family of even-symmetric polynomials indexed by the integer parameter $\mathcal{L} \geq 1$ in the form

$$\mathcal{P}_{\mathcal{L}}(z) = 1 + \sum_{n=1}^{\mathcal{L}} p_{\mathcal{L}}[2n-1](z^{-2n+1} + z^{2n-1}) \tag{6}$$

with odd-length $4\mathcal{L} - 1$, real even-symmetric coefficients $p_{\mathcal{L}}[n] = p_{\mathcal{L}}[-n]$ and $p_{\mathcal{L}}[2n] = 0$ for $n = \pm 1, \ldots, \pm\mathcal{L}$, and finite support $[-2\mathcal{L}+1, 2\mathcal{L}-1]$. Then $\mathcal{P}_{\mathcal{L}}(z)$ has $\mathcal{L}$ unique coefficients $c_{\mathcal{L}}[i] = p_{\mathcal{L}}[2i-1]$ for $i = 1, 2, \ldots, \mathcal{L}$.

[1] Conventional methods refer to those that are well developed, widely available, and broadly applicable. This definition excludes the asymptotic methods of Temme [51] for high order Daubechies polynomials.

According to Shensa [37], when the coefficients $c_{\mathcal{L}}[i]$ are computed as

$$c_{\mathcal{L}}[i] = \frac{\prod_{j\neq i}(j-1/2)}{\prod_{j\neq i}(j-i)} \tag{7}$$

for $j \in [-\mathcal{L}+1, \ldots, \mathcal{L}-1, \mathcal{L}]$, the resulting Lagrange polynomial $\mathcal{P}_{\mathcal{L}}(z)$, as a positive symmetric Laurent polynomial of degree $d_2 = 2\mathcal{L}-1$, interpolates exactly all regular polynomials of degree $d \leq 2\mathcal{L}-1$. This exact interpolation requires that the polynomial $\mathcal{P}_{\mathcal{L}}(z)$ be used as a halfband filter upscaling by rate $R = 2$ with filter normalization such that $p_{\mathcal{L}}[0] = 1$ and $\sum_n p_{\mathcal{L}}[n] = 2$.

Since the product $\mathcal{P}_{\mathcal{L}}(z)$ has a zero at $z = -1$ of multiplicity $2\mathcal{L}$, the other $2(\mathcal{L}-1)$ simple zeros can be collected in the quotient

$$\mathcal{Q}_{\mathcal{L}}(z) = \frac{\mathcal{P}_{\mathcal{L}}(z)}{(z+1)^{\mathcal{L}}(z^{-1}+1)^{\mathcal{L}}}. \tag{8}$$

This quotient $\mathcal{Q}_{\mathcal{L}}(z)$ is also a symmetric Laurent polynomial [15] which can be split into the "square root" factors $\mathcal{R}_{\mathcal{L}}(z)$ and $\mathcal{R}_{\mathcal{L}}(z^{-1})$ with $|\mathcal{R}_{\mathcal{L}}(\omega)|^2 = \mathcal{Q}_{\mathcal{L}}(\omega)$. Thus, factorize

$$\begin{aligned}
\mathcal{P}_{\mathcal{L}}(z) &= (z+1)^{\mathcal{L}}(z^{-1}+1)^{\mathcal{L}}\mathcal{Q}_{\mathcal{L}}(z) \\
&= (z+1)^{\mathcal{L}}\mathcal{R}_{\mathcal{L}}(z)(z^{-1}+1)^{\mathcal{L}}\mathcal{R}_{\mathcal{L}}(z^{-1}) \\
&= \mathcal{A}_{\mathcal{L}}(z)\mathcal{A}_{\mathcal{L}}(z^{-1})
\end{aligned}$$

neglecting normalization constants. The product filter $\mathcal{P}_{\mathcal{L}}(z)$ has thus been split into

$$\mathcal{A}_{\mathcal{L}}(z) = (z+1)^{\mathcal{L}}\mathcal{R}_{\mathcal{L}}(z) \tag{9}$$

$$\mathcal{S}_{\mathcal{L}}(z) = \mathcal{A}_{\mathcal{L}}(z^{-1}) \tag{10}$$

as the factors for the analysis and synthesis filters

For the Lagrange product polynomial $\mathcal{P}_{\mathcal{L}}(z)$ with $2\mathcal{L}$ zeros at $z = -1$ and length $4\mathcal{L}-1$ coefficients, this square root factorization generates the Daubechies analysis factor $\mathcal{A}_{\mathcal{L}}(z)$ with $\mathcal{L}$ zeros at $z = -1$ and length $2\mathcal{L}$ coefficients. When expressed in regular polynomial form, the Lagrange polynomial can be factored as

$$\mathcal{P}_{\mathcal{L}}(z) = (z+1)^{2\mathcal{L}} \prod_{i=1}^{n^{\mathrm{cq}}} \mathcal{U}(z; z_i) \prod_{j=1}^{n^{\mathrm{rd}}} \mathcal{V}(z; r_j) \tag{11}$$

$$\mathcal{U}(z; z_i) = (z-z_i)(z-z_i^{-1})(z-\bar{z}_i)(z-\bar{z}_i^{-1}) \tag{12}$$

$$\mathcal{V}(z; r_j) = (z-r_j)(z-r_j^{-1}) \tag{13}$$

where z_i and r_j are complex and real roots, and $n^{\mathrm{cq}} = \lfloor(\mathcal{L}-1)/2\rfloor$ and $n^{\mathrm{rd}} = (\mathcal{L}-1) \bmod 2$ are the numbers of complex quadruplets $\mathcal{U}(z; z_i)$ and real duplets $\mathcal{V}(z; r_j)$, respectively. When used as a filter with impulse response $p_{\mathcal{L}}[n]$ and frequency response $\mathcal{P}_{\mathcal{L}}(\omega)$, call it the Lagrange Real Nonorthogonal Symmetric Interpolating or LRNSI$(N; K; d)$ filter (Table 1) with parameters for length $N = 4\mathcal{L}-1$, number $K = 2\mathcal{L}$ of zeros at $z = -1$, and regular degree $d = 2\mathcal{L}-1$ of polynomials for which interpolation should be exact.

To compute the roots of $\mathcal{P}_{\mathcal{L}}(z)$ numerically, the companion matrix eigenvalue method (Section 2.1.1) can be used, and then those roots $z_k \approx -1$ can be replaced with $z_k = -1$. This substitution can be accomplished using either one of two methods: 1) given an error tolerance ϵ, subject all roots to the test $|z_k + 1| < \epsilon$ and replace those roots that pass the test, or 2) given the parameter $\mathcal{L}$ for the polynomial $\mathcal{P}_{\mathcal{L}}(z)$, sort all roots in increasing order of $|z_k + 1|$ and replace the first $2\mathcal{L}$ roots.

2.1.3 Daubechies Polynomials

The family of Daubechies polynomials $\mathcal{P}_{\mathcal{D}}(z)$ indexed by integer parameter $\mathcal{D} \geq 0$ can be factored in a manner analogous to the Lagrange polynomials $\mathcal{P}_{\mathcal{L}}(z)$. However, unlike the Lagrange coefficients $p_{\mathcal{L}}[n]$, the Daubechies coefficients $p_{\mathcal{D}}[n]$ cannot be computed explicitly, but instead must be computed from the roots. Express the Daubechies product polynomial $\mathcal{P}_{\mathcal{D}}(z)$ in the form

$$\mathcal{P}_{\mathcal{D}}(z) = (z+1)^{2(\mathcal{D}+1)} \mathcal{Q}_{\mathcal{D}}(z) \tag{14}$$

with the quotient polynomial $\mathcal{Q}_{\mathcal{D}}(z)$ a Laurent polynomial of degree $d_2 = \mathcal{D}$ with $2\mathcal{D}$ roots. Thus, $\mathcal{P}_{\mathcal{D}}(z)$ has $4\mathcal{D} + 2$ roots from which the $4\mathcal{D} + 3$ coefficients can be computed.

Consider mappings $x \to y \to z$ between three planes in the complex variables x, y, and z. Use the x plane to find the roots of the conditioned polynomial $\mathcal{C}_{\mathcal{D}}(x)$, map to the y plane for the roots of the binomial polymial $\mathcal{B}_{\mathcal{D}}(y)$, and map again to the z plane for the roots of the quotient polynomial $\mathcal{Q}_{\mathcal{D}}(z)$. All three polynomials $\mathcal{C}_{\mathcal{D}}(x)$, $\mathcal{B}_{\mathcal{D}}(y)$, and $\mathcal{Q}_{\mathcal{D}}(z)$ will be considered related forms of the product form $\mathcal{P}_{\mathcal{D}}(z)$ called the conditioned, binomial, and quotient forms, respectively.

The quotient form $\mathcal{Q}_{\mathcal{D}}(z)$ derives from division of the product form $\mathcal{P}_{\mathcal{D}}(z)$ by all of its roots at $z = -1$ as explained in Section 2.1.2 for the Lagrange polynomials. The binomial form ([6, Eq. 6.1.12], [36, Eq. 1], [15, Eq. 1.7])

$$\mathcal{B}_{\mathcal{D}}(y) = \sum_{i=0}^{\mathcal{D}} \binom{\mathcal{D}+i}{i} y^i \tag{15}$$

derives from the binomial series for $(1-y)^{-(\mathcal{D}+1)}$ truncated at $\mathcal{D}+1$ terms. To improve the numerical conditioning of the root finding problem for the roots y_i of $\mathcal{B}_{\mathcal{D}}(y)$, Shen and Strang [36] recommend the change of variables $x = \gamma y$ with $\gamma = 4$, while Goodman *et al.* [15] recommend the change of variables $x = 1/y$. Incorporating both transformations with $x = 1/(\gamma y)$, then

$$\begin{aligned}
\mathcal{B}_{\mathcal{D}}(y) &= \sum_{i=0}^{\mathcal{D}} \binom{\mathcal{D}+i}{i} y^i \\
&= (\gamma y)^{\mathcal{D}} \sum_{i=0}^{\mathcal{D}} \gamma^{-i} \binom{\mathcal{D}+i}{i} (\gamma y)^{i-\mathcal{D}} \\
&= x^{-\mathcal{D}} \mathcal{C}_{\mathcal{D}}(x)
\end{aligned}$$

yields the conditioned form

$$\mathcal{C}_{\mathcal{D}}(x) = \sum_{i=0}^{\mathcal{D}} \gamma^{-i} \binom{\mathcal{D}+i}{i} x^{\mathcal{D}-i}. \tag{16}$$

Now obtain the $\mathcal{D}$ roots x_i of $\mathcal{C}_{\mathcal{D}}(x)$ by computing the eigenvalues of the companion matrix. Then the $\mathcal{D}$ roots y_i of $\mathcal{B}_{\mathcal{D}}(y)$ can be calculated simply as $y_i = 1/(\gamma x_i)$.

With another change of variables $z + z^{-1} = 2 - 4y$ as used by Daubechies [5, 6], map the binomial $\mathcal{B}_{\mathcal{D}}(y)$, a regular polynomial with $\mathcal{D}$ roots, to the quotient $\mathcal{Q}_{\mathcal{D}}(z)$, a Laurent polynomial with $2\mathcal{D}$ roots. Given the Joukowski transformations [24, vol 1, pg 197, 223]

$$w = f(z) = (z + z^{-1})/2 \tag{17}$$

$$z = f^{-1}(w) = w \pm \sqrt{w^2 - 1} \tag{18}$$

and the affine transformations

$$y = g(w) = (1 - w)/2 \tag{19}$$

$$w = g^{-1}(y) = 1 - 2y, \tag{20}$$

the composite mappings[2] yield the explicit solutions

$$y = g(f(z)) = (1 - (z + z^{-1})/2)/2 \tag{21}$$

$$z = f^{-1}(g^{-1}(y)) = 1 - 2y \pm \sqrt{(1-2y)^2 - 1}. \tag{22}$$

The last equation $z = f^{-1}(g^{-1}(y))$ yields a doubly-valued solution with the reciprocal pair $\{z, z^{-1}\}$. When the pairs are regrouped as complex quadruplets $\{z, z^{-1}, \bar{z}, \bar{z}^{-1}\}$ and real duplets $\{r, r^{-1}\}$ and the polynomial expressed in regular form, $\mathcal{P}_{\mathcal{D}}(z)$ can be factored as

$$\mathcal{P}_{\mathcal{D}}(z) = (z+1)^{2(\mathcal{D}+1)} \prod_{i=1}^{n^{\mathrm{cq}}} \mathcal{U}(z; z_i) \prod_{j=1}^{n^{\mathrm{rd}}} \mathcal{V}(z; r_j) \tag{23}$$

where $n^{\mathrm{cq}} = \lfloor \mathcal{D}/2 \rfloor$ and $n^{\mathrm{rd}} = \mathcal{D} \bmod 2$ using notation analogous to that for the factorization of $\mathcal{P}_{\mathcal{L}}(z)$ in Section 2.1.2. When used as a filter with impulse response $p_{\mathcal{D}}[n]$ and frequency response $\mathcal{P}_{\mathcal{D}}(\omega)$, call it the Daubechies Real Nonorthogonal Symmetric Interpolating or DRNSI$(N; K; d)$ filter (Table 1) with parameters for length $N = 4\mathcal{D} + 3$, number $K = 2\mathcal{D} + 2$ of zeros at $z = -1$, and regular degree $d = 2\mathcal{D} + 1$ of polynomials for which interpolation should be exact.

2.2 Generation of Filter Coefficients

2.2.1 Discrete Impulse Response

Given the roots z_k of a degree d polynomial

$$\mathcal{F}(z) = \prod_{k=1}^{d} (z - z_k) \tag{24}$$

[2] Unlike other sections where f and g denote filters, here f and g denote functions that are conformal maps in the complex domain.

intended for use as a filter, the coefficients $\mathbf{f} \equiv f[n] \equiv f_n$ can be computed with an iterated convolution of factors of degree c. Express the polynomial as the product

$$\mathcal{F}(z) = \left(\prod_{k=Cc+1}^{d} (z - z_k) \right) \prod_{i=0}^{C-1} \left(\prod_{k=ic+1}^{ic+c} (z - z_k) \right) \tag{25}$$

of $C = \lfloor d/c \rfloor$ factors of degree c for roots $\{z_1, \ldots, z_{Cc}\}$ and an additional factor of degree $b = d \bmod c$ for roots $\{z_{Cc+1}, \ldots, z_d\}$. The additional factor is required only if d is not divisible by c. An actual algorithm can be implemented recursively [46]. When $c = 1$ with iterated convolution of linear factors, this algorithm reduces to one equivalent to Horner's method [17, pg 104].

A complete specification also requires fixing the order of the roots in the recursion. For example, if there is a factor of degree b in addition to those of degree c, its placement in the sequence must be determined by some specified order. Choices of c studied here include $c = 4$ with roots grouped by conjugate reciprocal quadruplets, $c = 2$ with roots paired as conjugates or reciprocals, and the conventional $c = 1$. Sort orders investigated include both increasing and decreasing absolute values as well as the Edrei-Leja order [12, 21]. The latter is defined by choosing

$$z_1 = \operatorname*{argmax}_{z_i} |z_i| \tag{26}$$

for the first root $k = 1$, and then

$$z_k = \operatorname*{argmax}_{z_i} \prod_{j=1}^{k-1} |z_i - z_j| \tag{27}$$

for the subsequent roots $k = 2, \ldots, d$. See [31, 32, 18] for other applications and discussion of the Edrei-Leja order.

Finally, the scaling of the coefficients must be fixed. Assume that an arbitrary filter $\mathbf{g}$ of length $N = d + 1$ coefficients has been computed from d roots of a polynomial. Alternatively, assume that an arbitrary $N \times M$ filter bank $\mathbf{G} \equiv [\mathbf{g}_0, \ldots, \mathbf{g}_{M-1}]$ has been given with a lowpass filter $\mathbf{g}_0$ such that $\sum_n g_0[n] \neq 0$. Then given a normalization constant η for the desired $\mathbf{F}$ to be obtained from the given $\mathbf{G}$, compute the η-normalized $\mathbf{F}$ with

$$\mathbf{f}_m = \left(\eta / \sum_{n=0}^{N-1} g_0[n] \right) \mathbf{g}_m \tag{28}$$

for $m = 0, 1, \ldots, M - 1$ which yields the desired constant $\eta = \sum_n f_0[n]$ as coefficient sum for the lowpass filter $\mathbf{f}_0$.

2.2.2 Continuous Impulse Response

Given an η-normalized $N \times 2$ filter bank $\mathbf{F}$, for notational convenience in this section, assume that $\mathbf{f}_0 \equiv \mathbf{f}$ is a lowpass scalet and $\mathbf{f}_1 \equiv \mathbf{h}$ is a highpass wavelet with the relation between $\mathbf{f}$ and $\mathbf{h}$ defined in Section 2.2.3. Then the coefficients $\mathbf{f}$ and $\mathbf{h}$ themselves constitute the discrete impulse responses for these FIR filters. Iterative interpolation with upscaling approximation yields

estimates of the continuous impulse responses for the scalet and wavelet functions corresponding to the scalet and wavelet filters. For the iterates $\{f^{(j)}[n]|j = 0, 1, 2, \dots\}$ of the scalet filter $f[n]$, let $f^{(0)}[n] = f[n]$ be the initial discrete impulse response and let

$$f^{(j+1)}[n] = \sum_{k=0}^{N-1} f[k] f^{(j)}[n - 2k] \tag{29}$$

determine the sequential estimates $\mathbf{f}^{(j)}$ of the continous impulse response approximating the corresponding scalet function

$$\phi(t) = \sum_{k=0}^{N-1} f[k] \phi(2t - k) \tag{30}$$

defined by an implicit two-scale equation relating ϕ to itself. Analogously, for the iterates $\{h^{(j)}[n]|j = 0, 1, 2, \dots\}$ of the wavelet filter $h[n]$, let $h^{(0)}[n] = h[n]$ be the initial discrete impulse response and let

$$h^{(j+1)}[n] = \sum_{k=0}^{N-1} h[k] f^{(j)}[n - 2k] \tag{31}$$

determine the sequential estimates $\mathbf{h}^{(j)}$ of the continous impulse response approximating the corresponding wavelet function

$$\psi(t) = \sum_{k=0}^{N-1} h[k] \phi(2t - k) \tag{32}$$

defined by an explicit two-scale equation relating ψ to ϕ. After J iterations, obtain the approximations $\phi(t_n) \approx \mathbf{f}^{(J)} \equiv f^{(J)}[n]$ and $\psi(t_n) \approx \mathbf{h}^{(J)} \equiv h^{(J)}[n]$ with discrete samples indexed by n at continuous times $t_n = n2^{-J-1}$.

2.2.3 Reconstructing Filter Banks

Quadrature mirror filter (QMF) and conjugate quadrature filter (CQF) banks were introduced by Esteban and Galand [13] and Smith and Barnwell [39], respectively. Different definitions with distinct conventions for sign, phase, and norm have been used for QMF and CQF banks by various authors in their software, papers, and books [6, 1, 52, 14, 41]. However, these filter bank conventions can be established using clearly specified principles. The primary guiding principles for the choices adopted here include: norm by symmetric distribution of normalization constants between analysis and synthesis filters, phase for the analysis lowpass filter by minimaxity of group delay (Section 2.4), and sign for the analysis highpass filter by positivity of sign (odd parity) in the definition of the CQF as the paraconjugate of the QMF.

To insure perfect reconstruction in 2-band filter banks with a symmetric distribution of normalization constants between both analysis and synthesis filters, we require $\eta = \sqrt{2}$. Thus, given the $\sqrt{2}$-normalized lowpass filter $\mathbf{f}$, let the corresponding highpass QMF

$$\mathbf{g} = \mathrm{qmf}(\mathbf{f}, p) \tag{33}$$

with parity $p \in \{0, 1\}$ be defined as

$$g_n = (-1)^{n+1+p} f_n \tag{34}$$

for $n = 0, \ldots, N-1$. With this notation and convention, then even parity $p = 0$ negates even-indexed coefficients $f[2i]$ while odd parity $p = 1$ negates odd-indexed coefficients $f[2i+1]$. Choosing $p = 1$ or $p = 0$ corresponds to a definition of a QMF in the z domain for which given $\mathcal{H}(z)$, the QMF is either $+\mathcal{H}(-z)$ or $-\mathcal{H}(-z)$, respectively. These alternative definitions imply negating coefficients of either odd or even powers of z. Thus, the definitions with either odd or even parity for p can also be designated the definitions with either positive or negative signs for $\mathcal{H}$, respectively. Taking $\mathbf{f}$ and $\mathbf{g}$ as column vectors, the QMF analysis and synthesis banks

$$\mathbf{A} = [\mathbf{a}_0, \mathbf{a}_1] = [\mathbf{f}, \mathbf{g}] \tag{35}$$

$$\mathbf{S} = [\mathbf{s}_0, \mathbf{s}_1] = [\mathbf{f}, -\mathbf{g}] \tag{36}$$

can then be constructed with $\mathbf{a}_0$ and $\mathbf{s}_0$ the analysis and synthesis lowpass band filters, and $\mathbf{a}_1$ and $\mathbf{s}_1$ the analysis and synthesis highpass band filters. However, a pair of analysis and synthesis filter banks $\mathbf{A}$ and $\mathbf{S}$ constructed in this manner does *not* yield a perfect reconstructing filter bank (PRFB) system.

Analogously, given the $\sqrt{2}$-normalized lowpass filter $\mathbf{f}$, let the corresponding highpass CQF be defined as the paraconjugate of the highpass QMF. Thus,

$$\mathbf{h} = \mathrm{cqf}(\mathbf{f}, p) \equiv [\mathrm{qmf}(\mathbf{f}, p)]^{\mathrm{P}} \tag{37}$$

with the CQF analysis and synthesis banks constructed as

$$\mathbf{A} = [\mathbf{a}_0, \mathbf{a}_1] = [\mathbf{f}, \mathbf{h}] \tag{38}$$

$$\mathbf{S} = [\mathbf{s}_0, \mathbf{s}_1] = [\mathbf{f}^{\mathrm{P}}, \mathbf{h}^{\mathrm{P}}] = \mathbf{A}^{\mathrm{P}} \tag{39}$$

which does yield a PRFB system.[3] Both the non-reconstructing QMFB system and the perfect reconstructing CQFB system can be built from a single orthogonal filter. However, the QMFB and CQFB systems yield, respectively, nonorthogonal and orthogonal filter banks. A perfect reconstructing system can also be built from two biorthogonal filters to yield a biorthogonal filter bank. Given biorthogonal lowpass filters $\mathbf{a}$ of length N_a and $\mathbf{s}$ of length N_s from spectral factorization of a product $\mathbf{p}$, then let $N = \max(N_a, N_s)$ and $q = N \bmod 2$. Construct the analysis and synthesis banks with column vector zero padding as

$$\mathbf{A} = [\mathbf{a}_0 \mid \mathbf{a}_1] = \left[\begin{array}{c|c} \mathbf{a} & \mathrm{qmf}(\mathbf{s}, 1-p) \\ \mathbf{0}_{N+q-N_a} & \mathbf{0}_{N+q-N_s} \end{array}\right] \tag{40}$$

$$\mathbf{S} = [\mathbf{s}_0 \mid \mathbf{s}_1] = \left[\begin{array}{c|c} \mathbf{0}_q & \mathbf{0}_q \\ \mathbf{s} & \mathrm{qmf}(\mathbf{a}, p) \\ \mathbf{0}_{N-N_s} & \mathbf{0}_{N-N_a} \end{array}\right] \tag{41}$$

[3] Let $\mathbf{X}^{\mathrm{T}}$ and $\mathbf{X}^{\mathrm{H}} \equiv \bar{\mathbf{X}}^{\mathrm{T}}$ denote, respectively, the usual transpose and Hermitian (or conjugate transpose), while $\mathbf{X}^{\mathrm{R}} \equiv \mathbf{J}\mathbf{X}$ and $\mathbf{X}^{\mathrm{P}} \equiv \mathbf{J}\bar{\mathbf{X}}$ denote, respectively, the reverse and paraconjugate (or conjugate reverse) with counter-identity $\mathbf{J}$.

which yields a biorthogonal PRFB system.

2.3 Evaluation of Filter Parameters

2.3.1 Coefficient and Root Errors

Given a degree d polynomial with corresponding roots z_k and coefficients f_n,

$$\mathcal{F}(z) = \prod_{k=1}^{d}(z - z_k) = \sum_{n=0}^{d} f_n z^n \tag{42}$$

we need a measure of the accuracy of the coefficient and root representations relative to each other. If we assume that the coefficients are given as exact, then we can compute the error of the roots by a test on the roots or by reconstruction of the coefficients from the roots.

Temme [51] proposed tests of the relations

$$-f_{d-1} = f_d \sum_{k=1}^{d} z_k \tag{43}$$

$$(-1)^d f_0 = f_d \prod_{k=1}^{d} z_k \tag{44}$$

in order to avoid errors introduced by any instabilities in the reconstruction of the coefficients. Specify the sort order of the roots and reexpress these relations as the sorted roots error

$$\mathrm{sre}(\mathcal{F}) = \max\{|f_{d-1} + f_d \sum_{k=1}^{d} z_k|, |(-1)^d f_0 - f_d \prod_{k=1}^{d} z_k|\} \tag{45}$$

defined as the maximum of the two absolute values.

Goodman *et al.* [15, Eq. 3.3] used an ℓ^2 norm on the relative error values of the coefficients. However, to account for coefficients that are possibly near zero, it is necessary to use mixed error values of the coefficients. Thus, using the more general ℓ^p norm with the mixed error values, this reconstructed coefficient error can be expressed as

$$\mathrm{rce}(\mathcal{F}; p) = \left[\sum_{n=0}^{d} \left(\frac{|f_n - \hat{f}_n|}{|f_n| + 1}\right)^p\right]^{1/p} \tag{46}$$

where $\hat{f}_n$ are the coefficients reconstructed from the roots z_k.

As filter parameters characterizing the relation between the set of coefficients and roots, we can report both $\mathrm{sre}(\mathcal{F})$ and $\mathrm{rce}(\mathcal{F})$ errors individually. Alternatively, denote the maximum of the pair of error values as a more "conservative" parameter estimating the coefficients and roots error

$$\mathrm{cre}(\mathcal{F}; p) = \max\{\mathrm{rce}(\mathcal{F}; p), \mathrm{sre}(\mathcal{F})\} \tag{47}$$

which would then reflect a numerical instability in the conversion from either root or coefficient domain to the other. All values reported here for both $\mathrm{rce}(\mathcal{F}; p)$ and $\mathrm{cre}(\mathcal{F}; p)$ were computed with $p = 1$. As a consequence, $\mathrm{rce}(\mathcal{F}; p)$ and $\mathrm{cre}(\mathcal{F}; p)$ are denoted simply as $\mathrm{rce}(\mathcal{F})$ and $\mathrm{cre}(\mathcal{F})$.

2.3.2 M^{th}-Band Interpolation Error

Define an Mth-band interpolation filter as a lowpass filter $\mathbf{f}$ such that the coefficients $f[n]$ and peak magnitude coefficient $f[\tau]$ at time index $n = \tau$ satisfy one of the three alternative sum conditions

$$\sum_n f[n] = \begin{cases} M & \text{if } f[\tau] = 1 \\ M^{1/2} & \text{if } f[\tau] = M^{-1/2} \\ 1 & \text{if } f[\tau] = M^{-1} \end{cases} \tag{48}$$

together with the following zero constraint

$$f[\tau \pm iM] = 0 \tag{49}$$

for $i = \{1, 2, 3, \dots\}$ sufficient to cover the entire length of the filter. Exact interpolation requires the filter to be normalized according to the first of the three sum conditions.

Given this definition for an Mth-band interpolation filter $\mathbf{f}$, we can numerically test $\mathbf{f}$ for its Mth-band interpolation error ε_{i} with the function mie($\mathbf{f}$) according to the following sequence of definitions:

$$\tau = \underset{n}{\operatorname{argmax}} |f[n]| \tag{50}$$

$$v = \underset{y}{\operatorname{argmin}} |y - f[\tau]| : y \in \{1, M^{-1/2}, M^{-1}\} \tag{51}$$

$$\varepsilon_{\text{i}} = \text{mie}(\mathbf{f}) \equiv \max\{|v - f[\tau]|, |f[\tau \pm iM]|, |Mv - \sum_n f[n]|\} \tag{52}$$

where the subscript i in ε_{i} denotes interpolation. Here the value ε_{i} is determined as the maximum of the absolute values from the tests of the central coefficient, required zeros, and coefficient sum.

This more general test permits some flexibility allowing for up to three different normalizations of the interpolation filter. However, restricting the test to just one of the three normalizations provides a more specific standardized test. Thus, all values ε_{i} of the function mie($\mathbf{f}$) reported here were computed for the filter normalization with $1 = f[\tau]$ and $2 = M = \sum_n f_n$ enabling exact interpolation.

2.3.3 Phase NonLinearity

With regard to the phase contribution for the filter root complex conjugate duplet $\{z_k, \bar{z}_k\}$ selected from the quadruplet $\{z_k, \bar{z}_k, z_k^{-1}, \bar{z}_k^{-1}\}$, Daubechies [6, pg. 255] provided a derivation for the formula

$$\Phi_{\text{cc}}(\omega; z_k) = \arctan\left[\frac{(r_k^2 - 1)\sin(\omega)}{(r_k^2 + 1)\cos(\omega) - 2r_k\cos(\alpha_k)}\right] \tag{53}$$

where her notation has been modified here with use of $z_k = r_k e^{i\alpha_k}$ and the subscript cc denotes complex conjugates. For the real root $z_l = r_l$ selected from the reciprocal duplet $\{z_l, z_l^{-1}\}$, she gave

$$\Phi_{\text{rs}}(\omega; z_l) = \arctan\left[\frac{r_l + 1}{r_l - 1}\tan(\omega/2)\right] \tag{54}$$

as the formula for the phase contribution, here with subscript rs denoting real singlets. Her method was extended by Taswell [45] with an analogous derivation for the phase contribution from the complex reciprocal duplet $\{z_j, z_j^{-1}\}$ selected from the quadruplet $\{z_j, \bar{z}_j, z_j^{-1}, \bar{z}_j^{-1}\}$ resulting in the formula

$$\Phi_{\mathrm{cr}}(\omega; z_j) = \arctan\left[\frac{(r_j - r_j^{-1})\sin(\alpha_j)}{(r_j + r_j^{-1})\cos(\alpha_j) - 2\cos(\omega)}\right] \tag{55}$$

with the subscript cr denoting complex reciprocals.

Daubechies extracted the nonlinear component of each contribution by subtraction of the linear component [6, pg. 255] with the formula

$$\Psi(\omega) = \Phi(\omega) - \frac{\omega}{2\pi}\Phi(2\pi) \tag{56}$$

after first removing ("ironing out") jump discontinuities in $\Phi(\omega)$ by choosing the continuous valuation of arctan over the interval $[0, 2\pi]$ such that $\arctan(0) = 0$. While appropriate for the real filters examined by Daubechies, this interval must be shifted to $[-\pi, \pi]$ to account for spectral factors yielding either real or complex filters. Thus, redefine

$$\Psi(\omega) = \Phi(\omega) - \frac{\omega}{\pi}\Phi(\pi) \tag{57}$$

and compute the total nonlinear phase

$$\Upsilon(\omega) = \sum_{j=1}^{n^{\mathrm{cr}}} \Psi_{\mathrm{cr}}(\omega; z_j) + \sum_{k=1}^{n^{\mathrm{cc}}} \Psi_{\mathrm{cc}}(\omega; z_k) + \sum_{l=1}^{n^{\mathrm{rs}}} \Psi_{\mathrm{rs}}(\omega; z_l) \tag{58}$$

by summing the contributions from all roots (except those at $z = -1$). Here $0 \le n^{\mathrm{cr}} \le n^{\mathrm{cq}}/2$, $0 \le n^{\mathrm{cc}} \le n^{\mathrm{cq}}/2$, and $0 \le n^{\mathrm{rs}} \le n^{\mathrm{rd}}/2$ are the numbers of complex reciprocal duplets, complex conjugate duplets, and real singlets, while n^{cq} and n^{rd} are the numbers of complex quadruplets and real duplets defined in both Sections 2.1.2 and 2.1.3 for the Lagrange and Daubechies polynomials. For filters designed by typical selection criteria as explained in Section 2.4, n^{cr} and n^{cc} are not both simultaneously nonzero, whereas nonzero n^{rs} may occur for either nonzero n^{cr} or n^{cc}.

Given the filter $\mathcal{F}(z)$ specified by its roots, we can now define its phase nonlinearity as the $L^p[-\pi, \pi]$ integral of $\Upsilon(\omega)$. Thus,

$$\varphi = \mathrm{pnl}(\mathcal{F}; p) \equiv \left(\int_{-\pi}^{\pi} |\Upsilon(\omega)|^p \, d\omega\right)^{1/p} \tag{59}$$

with a discrete sum approximation computed by trapezoidal or other quadrature rule. By default, assume that $p = 1$ for the $L^1[-\pi, \pi]$ integral.

2.3.4 Other Filter Parameters

All other filter parameters were computed as described by Taswell [48]. Parameters estimated include the time-domain regularity $\rho = \mathrm{tdr}(\mathcal{F})$, frequency-domain selectivity $\boldsymbol{\varsigma} = \mathrm{fds}(\mathbf{F})$, time-frequency uncertainty $\boldsymbol{\upsilon} = \mathrm{tfu}(\mathbf{F})$, vanishing moments numbers $\boldsymbol{\nu} = \mathrm{vmn}(\mathbf{F})$ (defined assuming

a tolerance of 1×10^{-4}), M-shift biorthogonality error $\varepsilon_{\mathrm{b}} = \mathrm{mbe}(\mathbf{A}, \mathbf{S})$, M-shift orthogonality error $\varepsilon_{\mathrm{o}} = \mathrm{moe}(\mathbf{F})$, and M-band reconstruction error $\varepsilon_{\mathrm{r}} = \mathrm{mre}(\mathbf{A}, \mathbf{S})$. All filter parameters are computed as empirical estimates with the exception of $\mathrm{tdr}(\mathcal{S})$ for the DRBSS family. Since $\mathrm{tdr}(\mathcal{F})$ is estimated with the roots $z_k \neq -1$ of $\mathcal{F}(z)$, and the set of such roots is empty for $\mathcal{S}(z)$ in the DRBSS family, $\mathrm{tdr}(\mathcal{S})$ was assigned the value K_s.

2.4 Selection of Spectral Factors

2.4.1 Factorization Rules

For an arbitrary polynomial $\mathcal{F}(z)$ with length N coefficients, there are $N-1$ roots of which $0 \leq K \leq N-1$ may be at $z=-1$. When considering spectral factorization, the product filter polynomial $\mathcal{P}_{\mathcal{D}}(z)$ with $N_p = 4\mathcal{D}+3$ coefficients and $K_p = 2\mathcal{D}+2$ roots at $z=-1$ is factored into the analysis and synthesis filter polynomials $\mathcal{A}(z)$ and $\mathcal{S}(z)$ with N_a and N_s coefficients, and K_a and K_s roots at $z=-1$, respectively. This factorization yields the constraints

$$N_p = N_a + N_s - 1 \tag{60}$$

$$K_p = K_a + Ks \tag{61}$$

on the lengths of the three filters and their roots at $z=-1$. Each family of filters has been named with an identifying acronym followed by $(N_a, N_s; K_a, K_s)$ in the biorthogonal cases and by $(N; K)$ in the orthogonal cases for which

$$N = N_a = N_s \tag{62}$$

$$K = K_a = K_s \tag{63}$$

is required. Tables 1 and 2 summarize the names and designs of the filter families.

With regard to the various cases of real biorthogonal, real orthogonal, and complex orthogonal, various additional constraints must be imposed. If K_a, K_s, and $K_p = K_a + K_s$ are the numbers of roots at $z=-1$ for $\mathcal{A}(z)$, $\mathcal{S}(z)$, and $\mathcal{P}(z)$, respectively, then the corresponding filters have coefficient lengths

$$N_a = K_a + 4n_a^{\mathrm{cq}} + 2n_a^{\mathrm{rd}} + 1 \tag{64}$$

$$N_s = K_s + 4n_s^{\mathrm{cq}} + 2n_s^{\mathrm{rd}} + 1 \tag{65}$$

$$N_p = 2K_p - 1 \tag{66}$$

where n_a^{cq}, n_s^{cq}, n_a^{rd}, and n_s^{rd} are the numbers of complex quadruplets $\{z, z^{-1}, \bar{z}, \bar{z}^{-1}\}$ and real duplets $\{r, r^{-1}\}$ for $\mathcal{A}(z)$ and $\mathcal{S}(z)$. Both n^{cq} and n^{rd} may be whole or half integer. If half integer, then half a complex quadruplet denotes a complex duplet while half a real duplet denotes a real singlet.

For K_a and K_s necessarily both odd or both even, then K_p is always even and $K = K_p/2$ a whole integer determines $n_p^{\mathrm{cq}} = n_a^{\mathrm{cq}} + n_s^{\mathrm{cq}}$ and $n_p^{\mathrm{rd}} = n_a^{\mathrm{rd}} + n_s^{\mathrm{rd}}$ according to $n_p^{\mathrm{cq}} = \lfloor (K-1)/2 \rfloor$ and $n_p^{\mathrm{rd}} = (K-1) \bmod 2$. If K_a and K_s are given, then K_p and K yield n_p^{cq} and n_p^{rd} split into $\{n_a^{\mathrm{cq}}, n_a^{\mathrm{rd}}\}$

and $\{n_s^{\mathrm{cq}}, n_s^{\mathrm{rd}}\}$ and the roots are factored accordingly. For real coefficients, a root z must be paired with its conjugate $\bar{z}$. For symmetric coefficients, a root z must be paired with its reciprocal z^{-1}. For 2-shift orthogonal coefficients, a root z must be *separated* from its conjugate reciprocal $\bar{z}^{-1}$.

Thus, in the real biorthogonal symmetric case, each complex quadruplet $\{z, \bar{z}, z^{-1}, \bar{z}^{-1}\}$ and real duplet $\{r, r^{-1}\}$ must be assigned in its entirety to either $\mathcal{A}(z)$ or $\mathcal{S}(z)$. In the real orthogonal case, each complex quadruplet is split into two conjugate pairs $\{z, \bar{z}\}$ and $\{z^{-1}, \bar{z}^{-1}\}$, while each real duplet is split into two singlets $\{r\}$ and $\{r^{-1}\}$, with one factor assigned to $\mathcal{A}(z)$ and the other to $\mathcal{S}(z)$. The complex orthogonal case is analogous to the real orthogonal case except the complex quadruplets are split into reciprocal pairs $\{z, z^{-1}\}$ and $\{\bar{z}, \bar{z}^{-1}\}$ instead of conjugate pairs. The complex orthogonal symmetric case requires use of complex quadruplets without real duplets.

All orthogonal cases require $K = K_a = K_s = K_p/2$, $n_a^{\mathrm{cq}} = n_s^{\mathrm{cq}} = n_p^{\mathrm{cq}}/2$, and $n_a^{\mathrm{rd}} = n_s^{\mathrm{rd}} = n_p^{\mathrm{rd}}/2$ with $N = N_a = N_s = 2K$. Note that n_p^{rd} can only equal 0 or 1. Therefore, in biorthogonal cases, either $\{n_a^{\mathrm{rd}} = 0,\ n_s^{\mathrm{rd}} = 1\}$ or $\{n_a^{\mathrm{rd}} = 1,\ n_s^{\mathrm{rd}} = 0\}$. However, in orthogonal cases, either $\{n_a^{\mathrm{rd}} = n_s^{\mathrm{rd}} = 0\}$ or $\{n_a^{\mathrm{rd}} = n_s^{\mathrm{rd}} = 1/2\}$ with 1/2 of a duplet denoting a singlet. For all real orthogonal cases as well as complex orthogonal cases not involving symmetry criteria, K can be any positive integer. For the complex orthogonal least-asymmetric and most-asymmetric cases, K must be a positive even integer. For the complex orthogonal least-symmetric and most-symmetric cases, K must be a positive odd integer.

For real biorthogonal symmetric cases, K_a and K_s must be both odd or both even. In the biorthogonal symmetric spline case, all additional roots (other than those at $z = -1$ with assignment determined by K_a and K_s) are assigned to $\mathcal{A}(z)$ leaving $\mathcal{S}(z)$ as the spline filter. All other biorthogonal symmetric cases incorporate a root assignment constraint that balances the lengths of the analysis and synthesis filters such that $N_a \approx N_s$ as much as possible. Thus, the lengths N_a (Eq. 64) and N_s (Eq. 65) are balanced with $n_a^{\mathrm{cq}},\ n_s^{\mathrm{cq}},\ n_a^{\mathrm{rd}},\ n_s^{\mathrm{rd}}$ determined with the following pseudocode:

```
n_a^cq = 0;  n_s^cq = 0;
if n_p^cq;
    if K_s > K_a;  n_a^cq = ⌊K_s/4⌋; n_s^cq = n_p^cq − n_a^cq;
    elseif K_a > K_s; n_s^cq = ⌊K_a/4⌋; n_a^cq = n_p^cq − n_s^cq;
    else; n_a^cq = ⌈n_p^cq/2⌉; n_s^cq = n_p^cq − n_a^cq; end;
end;
n_a^rd = 0;  n_s^rd = 0;
if n_p^rd;
    if K_s + 4 * n_s^cq >= K_a + 4 * n_a^cq;  n_a^rd = 1;
    else; n_s^rd = 1; end;
end;
```

For $K_a = 2i - 1$ and $K_s = 2j - 1$ both odd with $i, j \in \{1, 2, 3, \ldots\}$, balancing of equal filter lengths is possible. In fact, requiring *both* $K_a = K_s$ *and* $N_a = N_s$ is also possible when $N = N_a = N_s = 2K$

with $K = K_a = K_s$ for $\{K = 1 + 4k \mid \ k = 1, 2, 3 \ldots\}$. However, for $K_a = 2i$ and $K_s = 2j$ both even, equal balancing of filter lengths N_a and N_s is not possible. The additional unbalanced roots are assigned to $\mathcal{A}(z)$ such that $N_a > N_s$ leaving $\mathcal{S}(z)$ as the shorter filter.

2.4.2 Selection Criteria

Simple geometric rules are used as selection criteria for the three families *not* subjected to a combinatorial optimization search. Thus, the DRBSS, DROMD, and DCOMD families assign, respectively, all roots $\{z_j \neq -1\}$, $\{z_j = r_j e^{i\alpha_j} \mid r_j < 1\}$, and $\{(z_j, z_j^{-1}) \mid r_j < 1, \alpha_j \geq 0\}$ to $\mathcal{A}(z)$. The DROMD family, which is real and orthogonal, has been called "extremal phase" [5] and "least delayed" [50]. It has been renamed here for consistency with the DCOMD family, which is complex and orthogonal. For both DROMD and DCOMD families, the MD for "most disjoint" refers to the geometric separability of the root sets for $\mathcal{A}(z)$ and $\mathcal{S}(z)$ with the simplest topology.

Numerical estimates of defined filter parameters are used as selection criteria for all other families subjected to optimization. These criteria include $\mathrm{pnl}(\mathcal{A})$, $\mathrm{tdr}(\mathcal{A})$, $\mathrm{fds}(\mathcal{A})$, and $\mathrm{tfu}(\mathcal{A})$ (Section 2.3.4). Most of the orthogonal families are defined by $\mathrm{pnl}(\mathcal{A})$ selecting for varying degrees of asymmetry or symmetry (Section 2.3.3). Previous work [45, 50] has been revised by the shift of the integration interval for $\mathrm{pnl}(\mathcal{A})$ from $[0, 2\pi]$ to $[-\pi, \pi]$ and by the use of $\mathrm{pnl}(\mathcal{A})$ as a "tie-breaker" criterion for root subsets in families optimized by the other criteria. These revisions now insure unique criterion values for each root subset examined in the combinatorial search. The complexity of the search can be reduced by ignoring binary complements of coded root subsets for orthogonal families in all cases as long as the final selected root subset is subjected to a comparison test to choose the primary versus the complementary. The necessity to choose between the primary and complementary coded subsets for biorthogonal families occurs only for cases when $K_a = K_s$, $n_a^{\mathrm{cq}} = n_s^{\mathrm{cq}}$, and $n_a^{\mathrm{rd}} = 0 = n_s^{\mathrm{rd}}$ all hold true.

Minimizing or maximizing $\mathrm{pnl}(\mathcal{A})$ for real filters defines DROLA and DROMA, respectively, the least and most asymmetric families. If the parity of K is ignored, then minimizing or maximizing $\mathrm{pnl}(\mathcal{A})$ for complex filters defines DCOLN and DCOMN, respectively, the least and most nonlinear families. Phase nonlinearity does not exist and cannot be used for the biorthogonal families all of which are real and symmetric. Therefore, one of the other filter parameters must be used as an optimization criterion to select the spectral factors for these symmetric families. In addition, these biorthogonal families are subjected to the length constraints determined by the principle of balancing the filter lengths for both $\mathcal{A}(z)$ and $\mathcal{S}(z)$ as described in Section 2.4.1.

For all but one of the families subjected to a combinatorial search, the selection criterion is optimized for the analysis filter. The DRBBR family is the exception where the selection criterion is optimized for both analysis and synthesis filters by maximizing a balancing measure B defined as

$$B(\mathrm{tdr}(\cdot), \mathcal{A}, \mathcal{S}) = \left| \frac{\mathrm{tdr}(\mathcal{A}) + \mathrm{tdr}(\mathcal{S})}{\mathrm{tdr}(\mathcal{A}) - \mathrm{tdr}(\mathcal{S})} \right| \tag{67}$$

when applied to $\mathrm{tdr}(\cdot)$ for $\mathcal{A}$ and $\mathcal{S}$. In this case, an exception is also made to the primary subset

versus complementary subset comparison rules (Section 2.4.3). After balancing the regularities for both $\mathcal{A}$ and $\mathcal{S}$, the final selection is chosen so that $\mathrm{tdr}(\mathcal{S}) > \mathrm{tdr}(\mathcal{A})$.

Table 2 summarizes the filter designs for the families. Note that the DCOLN family is the union of the even-indexed DCOLA and odd-indexed DCOMS families, while the DCOMN family is the union of the even-indexed DCOMA and odd-indexed DCOLS families. Also, two pairs of families are computed via different algorithms but should ideally be equivalent, and thus provide a test for verifying computational methods. The DROMD and DROMA families should be equivalent real families, while the DCOMD and DCOMN families should be equivalent complex families.

2.4.3 Unifying Algorithm

All filter families of the systematized collection are generated by the spectral factorization and optimizing combinatorial search incorporated in the following algorithm which has been implemented in MATLAB and called `fcdmlmf` for Filter Coefficients Daubechies Minimum Length Maximum Flatness:

1. Input the identifying name `FiltName` for the family of filters and the indexing design parameters K_a and K_s.

2. Compute $K_p = K_a + K_s$, $\mathcal{D} = K_p/2 - 1$, and the $n_p^{\mathrm{cq}} = \lfloor \mathcal{D}/2 \rfloor$ complex quadruplet and $n_p^{\mathrm{rd}} = \mathcal{D} \mod 2$ real duplet roots of the quotient filter $\mathcal{Q}_{\mathcal{D}}(z)$ (Section 2.1.3).

3. Determine the factorization rules and selection criterion that define the family of filters named `FiltName`.

4. Compute the splitting number pairs $\{n_a^{\mathrm{cq}}, n_s^{\mathrm{cq}}\}$ and $\{n_a^{\mathrm{rd}}, n_s^{\mathrm{rd}}\}$ from $\{n_p^{\mathrm{cq}}, n_p^{\mathrm{rd}}\}$ for the `FiltName` filter pair indexed by $\{K_a, K_s\}$.

5. Sort the roots in an order convenient for the class of splitting appropriate to the type of filter. All roots of a complex quadruplet should be adjacent with duplets of the quadruplet subsorted according to conjugates or reciprocals depending on the filter type. Assign binary coded labels 0 and 1 to the first and second duplet of each quadruplet. Analogously assign binary codes to the first and second singlet of the real reciprocal duplet if present. If biorthogonal, assign binary coded labels 0 or 1 to each of the entire quadruplets and duplets.

6. Generate the possible binomial subsets for these binary codes [33] subject to the imposed factorization rules and splitting numbers. For orthogonal filters, there are a total of $n_a^{\mathrm{cq}} + n_a^{\mathrm{rd}}$ binary selections without constraint on the bit sum, and thus $2^{n_a^{\mathrm{cq}}+n_a^{\mathrm{rd}}-1}$ binomial subsets ignoring complements. For biorthogonal filters, there are a total of n_p^{cq} binary selections with bit sum constrained to n_a^{cq}, and thus $\binom{n_p^{\mathrm{cq}}}{n_a^{\mathrm{cq}}}$ binomial subsets.

7. For each root subset selected by the binomial subset codes, characterize the corresponding filter by the optimization criterion appropriate for the `FiltName` family. These optimization

criteria may be any of the numerically estimated filter parameters computed from the roots or the coefficients (Section 2.3, also [48]).

8. Search all root subsets to find the one with the optimal value of the desired criterion. If necessary, apply the "tie-breaker" criterion.

9. Include the K_a and K_s required roots at $z = -1$ respectively for the selected optimal subset of roots intended for the spectral factor $\mathcal{A}(z)$ and for the complementary subset intended for the synthesis spectral factor $\mathcal{S}(z)$.

10. For orthogonal filters, compare the selected (primary) subset of filter roots and coefficients with its complementary subset to choose the one with minimax group delay over the interval $\omega \in [0, \pi]$ as the subset for $\mathcal{A}(z)$. For biorthogonal filters, compare the primary and complementary subsets only if $K_a = K_s$, $n_a^{\mathrm{cq}} = n_s^{\mathrm{cq}}$, and $n_a^{\mathrm{rd}} = 0 = n_s^{\mathrm{rd}}$ in order to choose the one with the defining criterion optimized for $\mathcal{A}(z)$.

After the filter roots have been selected for each of $\mathcal{A}(z)$ and $\mathcal{S}(z)$, the filter coefficients for the scalets and wavelets can be computed as explained in Section 2.2.1. Full searches of all possible combinatorial subsets should be performed for a sufficient number of K indices for the filter family's members to infer the appropriate pattern of binary codes with bit sums characterizing the family. Using such a pattern permits successful *partial* rather than *full* combinatorial searches. These partial searches provide significant reduction in computational complexity convenient for larger values of K (Section 4).

2.5 Hardware and Software

All results reported here were computed with Version 4.5b1 of the WAVBOX Software Library [42] running in Version 5.2.1 of the MathWorks MATLAB technical computing environment [25] on a Toshiba Tecra 720CDT with a 133 MHz Pentium CPU and the Microsoft Windows 95 operating system.

3 Results

3.1 Computation of Filter Roots

Figures 1 and 2 display the roots of the Daubechies polynomial $\mathcal{P}_{\mathcal{D}}(z)$ for $\mathcal{D} = 30$ and the impulse and frequency responses of its associated filter named DRNSI(123;62;61). Identical results (not shown) were obtained for the corresponding example with $\mathcal{L} = 31$ for the family of Lagrange polynomials $\mathcal{P}_{\mathcal{L}}(z)$ with associated filter named LRNSI($N; K; d$). This example demonstrates the equivalence of computational results for low order polynomials of the two families when $\mathcal{L} = \mathcal{D} + 1$. Recall that the family of polynomials $\{\mathcal{P}_{\mathcal{D}}(z) | \mathcal{D} = 0, 1, \ldots\}$ are indexed according to the number $\mathcal{D}$ of unique roots from which the coefficients are determined, while the family $\{\mathcal{P}_{\mathcal{L}}(z) | \mathcal{L} = 1, 2, \ldots\}$

are indexed according to the number $\mathcal{L}$ of unique symmetric coefficients from which the roots are determined.

To clarify further the distinction between LRNSI$(N;K;d)$ and DRNSI$(N;K;d)$ for given $(N;K;d)$, note that the coefficients of the filter LRNSI$(N;K;d)$ can be computed explicitly as the coefficients (Eq. 7) of the Lagrange polynomial $\mathcal{P}_{\mathcal{L}}(z)$. However, the coefficients of the filter DRNSI$(N;K;d)$ can only be computed indirectly via the roots of the conditioned form $\mathcal{C}_{\mathcal{D}}(x)$ (Eq. 16) or the binomial form $\mathcal{B}_{\mathcal{D}}(y)$ (Eq. 15) of the Daubechies polynomial $\mathcal{P}_{\mathcal{D}}(z)$. Either LRNSI$(N;K;d)$ or DRNSI$(N;K;d)$ can be used as the product filter for spectral factorization to obtain orthogonal and biorthogonal scalets and wavelets. Analytically, if $\mathcal{L} = \mathcal{D} + 1$, then ideally $\mathcal{P}_{\mathcal{L}}(z) = \mathcal{P}_{\mathcal{D}}(z)$ and LRNSI$(N;K;d)$ = DRNSI$(N;K;d)$ with equality of respective roots and coefficients. However, numerically, these relations hold true only for low order polynomials and filters.

For high order polynomials and filters, differences between the two families can be revealed clearly. For example, consider the case with $K = 200$ roots at $z = -1$ where bifurcations occurred in the root distribution patterns for both filters. However, the Mth-band interpolation errors (Eq. 52) differed dramatically with LRNSI(399;200;199) passing (mie$(\mathbf{p}_{\mathcal{L}}) = 6.7 \times 10^{-16}$) but DRNSI(399;200;199) failing (mie$(\mathbf{p}_{\mathcal{D}}) = 1.4 \times 10^{+11}$) this test. This difference reflects the instability in the computation of the coefficients from the roots for DRNSI. Moreover, the absence of a significant numerical value for the sorted roots error (Eq. 45) for either filter (sre$(\mathcal{P}_{\mathcal{L}}) = 1.0 \times 10^{-36}$ for LRNSI and inferred from sre$(\mathcal{C}_{\mathcal{D}}) = 3.6 \times 10^{-14}$ for DRNSI) does not insure the absence of a visually observeable bifurcation pattern in the root distribution. However, analytically in the absence of numerical error, there should be no bifurcation. Thus, Temme's root tests (Eq. 43, Eq. 44) implemented as the sorted roots error test (Eq. 45) may be necessary but not sufficient as a measure of the accuracy of the roots of a polynomial.

Figures 3 and 4 display examples of LRNSI and DRNSI with $K = 162$ where root bifurcation occured for LRNSI while coefficient instability occured for DRNSI. Again, in this case, neither the absence of a significant value for the sorted roots error nor the absence of a visually observeable bifurcation pattern in the roots for DRNSI insured the absence of an instability in the computation of the coefficients. Figure 2 displays an example of DRNSI with $K = 62$ where visually observeable root bifurcations and coefficient instabilities did not occur. Moreover, the errors sre$(\mathcal{P})$, rce$(\mathcal{P})$, and mie$(\mathbf{p})$ were all acceptably small (similarly for the comparable example of LRNSI, not shown). However, the vanishing moments numbers vmn$(\mathbf{p})$ did not approach the expected values. Analytically, vmn$(\mathbf{p}) = K$ is expected. Instead numerically, vmn$(\mathbf{p}_{\mathcal{L}=31}) = 14$ and vmn$(\mathbf{p}_{\mathcal{D}=30}) = 5$ were observed. These various examples demonstrate that the desired characteristic of a filter as reflected in a defined parameter must be tested directly in the appropriate domain of roots or coefficients.

Figure 5 provides a summary of the sorted root errors sre$(\mathcal{P})$ (Eq. 45) and the reconstructed coefficient errors rce$(\mathcal{P})$ (Eq. 46) for both the Lagrange $\mathcal{P}_{\mathcal{L}}(z)$ and Daubechies $\mathcal{P}_{\mathcal{D}}(z)$ polynomials corresponding to the sequence $\{K_p = 2i | i = 1, 2, \ldots, 100\}$ for the number of roots at $z = -1$. Root errors for the Daubechies sequence were computed for the indirect Daubechies conditioned form $\mathcal{C}_{\mathcal{D}}(x)$ (Eq. 16) whereas root errors for the Lagrange sequence were computed for the direct Lagrange form $\mathcal{P}_{\mathcal{L}}(z)$ (Eq. 7). The upper curves in each subplot represent the errors rce$(\mathcal{C}_{\mathcal{D}})$ and

rce($\mathcal{P}_{\mathcal{L}}$) while the lower curves represent the errors sre($\mathcal{C}_{\mathcal{D}}$) and sre($\mathcal{P}_{\mathcal{L}}$). Assuming a tolerance of 10^{-6} for the errors rce($\cdot$), the roots and coefficients can be computed and reconstructed accurately up to $K_p = 134$ ($\mathcal{L} = 67$)and $K_p = 74$ ($\mathcal{D} = 36$) for the Daubechies and Lagrange sequences, respectively.

3.2 Generation of Filter Coefficients

Alternative iterative convolution methods for computing filter coefficients from filter roots as explained in Section 2.2.1 were investigated for the DRNSI filters over a wide range of orders. Results [46] were scored both objectively with the Mth-band interpolation error mie($\mathbf{p}$) and subjectively with visual examination of the estimate of the continuous impulse response. At low order, all iterative convolution alternatives produced satisfactory and equivalent results. At high order, the convolution alternatives with Edrei-Leja order or with quadratic or quartic multiplier factors provided some stabilization but not sufficient to generate the correct impulse response for the half-band interpolation filter. Use of the convolution alternative with linear factors ($c = 1$ in Section 2.2.1) sorted in increasing absolute value order was chosen as the convention to generate all of the filters in the collection.

Figure 6 displays plots of estimates of the continous impulse and frequency responses for the lowpass scalet (dotted curves), highpass QMF wavelet (dashed curves), and highpass CQF wavelet (solid curves) for both even and odd parity ($p = 0$ and $p = 1$ in Section 2.2.3). The QMF and CQF wavelets have the same magnitude response but different phase responses, phase delays, and group delays. For each of the scalet, QMF wavelet, and CQF wavelet, the group delays are the same for both parities $p = 0$ and $p = 1$. However, the parity p does determine the location of the phase discontinuity in the phase response. In this example, for the CQF wavelet with $p = 0$, the discontinuities occur at $\omega = \pm\pi/2$ whereas with $p = 1$, they occur at $\omega = \pm\pi$ and at $\omega = 0$. Use of $p = 1$ was chosen as the convention to generate the filter collection.

3.3 Evaluation of Filter Parameters

Maximizing or minimizing the phase nonlinearity pnl($\mathcal{A}$) of the analysis factor $\mathcal{A}(z)$ served as a selection criterion to generate many of the filter families in the collection. Figures 7 and 8 display two examples of pnl($\mathcal{A}$) for $\mathcal{A}(z)$ selected respectively for DCOLA(12;6) and DCOMA(12;6) obtained from $\mathcal{P}_{\mathcal{D}}(z)$ with $\mathcal{D} = 5$. In these examples, there are two sets of complex duplets and one real singlet contributing to the phase nonlinearity. Computation of pnl($\mathcal{A}$) on the interval $[0, 2\pi]$ instead of $[-\pi, \pi]$ failed to discrimate properly between alternative root sets for these examples, and thus failed as a selection criterion yielding unique solutions. In contrast, use of the interval $[-\pi, \pi]$ provided a discriminating criterion confirmed by distinct values for each root set. In particular, for this example, the correct solution for DCOMA(12;6) was confirmed by comparison with DCOMD(12;6). Additional examples demonstrating computation of all of the various filter parameters used here as selection criteria can be found in [48].

3.4 Selection of Spectral Factors

To provide a complete pictorial representation of spectral factorization, a graphical array format has been devised with product $\mathcal{P}(z)$ and factors $\mathcal{A}(z)$ and $\mathcal{S}(z)$ in the rows, for each of which in the columns there are the roots, magnitude response, group delay response, and impulse response. Figures 9 and 10 display orthogonal and biorthogonal examples, respectively. The orthogonal example with DCOLA(12;6) in Figure 9 corresponds to the same example in Figure 7 with $\text{pnl}(\mathcal{A}) = 2.86$ the selected minimum. The biorthogonal example with DRBMS(17,15;8,8) in Figure 10 was selected with maximum $\text{fds}(\mathcal{A}) = 0.72$ when $\text{pnl}(\mathcal{A}) = 0$ for this symmetric family. Additional examples demonstrating spectral factorizations for all of the filter families with graphical displays in this format can be found in [46]. Figures 11 and 12 present visual comparisons of the distinct spectral factors selected for each of the real and complex orthogonal families at $K = 11$ and $K = 12$. In the subplots for roots, "o" and "x" represent the roots for $\mathcal{A}(z)$ and $\mathcal{S}(z)$, respectively. For each spectral factorization root set, there are two corresponding subplots for the analysis scalet and wavelet impulse responses. Real and imaginary parts of complex responses are shown in solid and dotted lines, respectively. Finally, to demonstrate the complete set of scalets and wavelets for a given family, Figures 13 and 14 display the DCOLN scalets and wavelets from $K = 1$ to $K = 24$. Technically, as listed in Table 2, complex filters for DCOLN require $K \geq 3$ because all orthogonal families are equivalent and real for $K \leq 2$. However, for consistency of comparisons with all other families (see below), graphical displays and numerical tables were arranged such that $K = 1$ and $K = 2$ were included.

3.5 Comparison of Filter Families

Using roots of the Daubechies polynomial $\mathcal{P}_{\mathcal{D}}(z)$ obtained with the conditioned form $\mathcal{C}_{\mathcal{D}}(x)$, all filters of all Daubechies biorthogonal and orthogonal families were verified to meet or surpass requirements for biorthogonality, orthogonality, and reconstruction when tested [48] in 2-band wavelet filter banks. In general, reconstruction errors ranged from "perfect" at $\mathcal{O}(10^{-16})$ to "near-perfect" at $\mathcal{O}(10^{-8})$ as $K = K_a = K_s$ ranged from $K = 1$ to $K = 24$ for both biorthogonal and orthogonal classes. The corresponding $K_p = 48$ for $K_a = K_s = 24$ remains well below the tolerance limit set at $K_p = 74$ with errors $\text{rce}(\cdot) < 10^{-6}$ for computation of the filters via the Daubechies conditioned form.

All filter families were observed to have the optimal values of their defining selection criterion when compared to the other families (Tables 3 to 8). Two examples are also displayed graphically with readily discernible visual patterns. An increasing linear trend appears for both DCOMN and DROMA families in Figure 15 which summarizes $\text{pnl}(\mathcal{A})$ for orthogonal filters. Although not as highly correlated, linear trends also appear for several of the families in Figure 16 which summarizes $\text{fds}(\mathbf{a}_0)$ and $\text{fds}(\mathbf{s}_0)$ for biorthogonal filters. The columns in the tables and the lists in the figure legends order the filter families according to the median values of the analysis filter parameter values observed for $1 \leq K \leq 24$. Additional figures for all parameters of all filter families can be found in [46].

Finally, Tables 9 and 10 list $\mathrm{vmn}(\mathbf{a}_1)$ and $\mathrm{vmn}(\mathbf{s}_1)$ for biorthogonal families and $\mathrm{vmn}(\mathbf{a}_1)$ for orthogonal families, respectively. The tables do not list $\mathrm{vmn}(\mathbf{a}_0)$ and $\mathrm{vmn}(\mathbf{s}_0)$ for the scalets. However, results were observed as follows: For biorthogonal scalets, $\mathrm{vmn}(\mathbf{a}_0) = 0$ and $\mathrm{vmn}(\mathbf{s}_0) = 0$ for odd K, while $\mathrm{vmn}(\mathbf{a}_0) = 2$ and $\mathrm{vmn}(\mathbf{s}_0) = 2$ for even K. For orthogonal scalets, $\mathrm{vmn}(\mathbf{a}_0) = 0$ for all K.

The DCOLS and DCOMS families have symmetric scalets and anti-symmetric wavelets, while DCOLA, DCOMA, DROLA, and DROMA have asymmetric scalets and wavelets. Combining the odd-indexed DCOMS and even-indexed DCOLA yields the union DCOLN = DCOMS ∪ DCOLA. Combining the odd-indexed DCOLS and even-indexed DCOMA yields the union DCOMN = DCOLS ∪ DCOMA. All have nonlinear group delays for both scalets and wavelets. The equivalences DROMA = DROMD and DCOMN = DCOMD were both confirmed for all K. For all filter families examined with indices in the range $2 \leq K \leq 24$ (that is, excluding the Haar filters at $K = 1$), the minimum $\mathrm{pnl}(\mathcal{A}) = 0.511$ occurs for DCOLN(46;23) while the maximum $\mathrm{pnl}(\mathcal{A}) = 52.244$ occurs for DCOMN(48;24). The second least value of $\mathrm{pnl}(\mathcal{A}) = 0.564$ occurs for DROLA(10;5) = DROLU(10;5).

$K = 6$ is the minimum K for which $\mathrm{tdr}(\mathcal{A}) \geq 2$. At $K = 6$, the maximum $\mathrm{tdr}(\mathcal{A}) = 2.244$ occurs for DROMR(12;6) and the minimum $\mathrm{tfu}(\mathcal{A}) = 0.694$ occurs for DROLU(12;6) = DROLA(12;6). $K = 9$ is the minimum K for which $\mathrm{tdr}(\mathcal{A}) \geq 3$. At $K = 9$, the maximum $\mathrm{tdr}(\mathcal{A}) = 3.161$ occurs for DCOMR(18;9) = DCOMN(18;9) and the minimum $\mathrm{tfu}(\mathcal{A}) = 0.795$ occurs for DCOLU(18;9) = DCOLN(18;9). $K = 13$ is the minimum K for which $\mathrm{tdr}(\mathcal{A}) \geq 4$. At $K = 13$, the maximum $\mathrm{tdr}(\mathcal{A}) = 4.106$ occurs for DCOMR(26;13) and the minimum $\mathrm{tfu}(\mathcal{A}) = 0.847$ occurs for DROLU(26;13). These examples demonstrate that for a given value of K and a given filter parameter the optimal value does not necessarily occur consistently for either the real or complex family.

As a final observation, for orthogonal filters, $K = 11$ is the minimum K for which the filters from all of the defined families are each distinct from one another for the given value of K (excluding the equivalence for all K of the two pairs of families DROMD = DROMA and DCOMD= DCOMN). Analogously, for biorthogonal filters, $K = 12$ is the minimum $K = K_a = K_s$ for which filters from all families are distinct for the given K.

4 Discussion

Computational algorithms have been developed for generating a systematized collection of Daubechies compact wavelets with a unifying algorithm incorporating filter design via spectral factorization of the Daubechies polynomial. These wavelet filters have minimum length and maximum flatness as well as any of a variety of other desired filter characteristics chosen for optimization. Criteria investigated include time-domain regularity, frequency-domain selectivity, time-frequency uncertainty, and phase nonlinearity (Tables 1 and 2).

Empirical estimates of these filter parameters have been used in conjunction with spectral factorization and combinatorial search methods to unify all of the diverse families of real and complex

orthogonal and biorthogonal Daubechies wavelets with a single algorithm (Section 2.4.3). This automated algorithm is valid for any order K of Daubechies wavelet subject to certain tolerances (see below) and insures that the same consistent choice of roots is always made in the computation of the filter coefficients. It is also sufficiently flexible and extensible that it can be generalized to select roots for filters optimized by (possibly weighted) combinations of criteria other than those investigated here.

The important criterion of phase nonlinearity has been used to design wavelet filters with varying degrees of symmetry or asymmetry. The terms "symmetric" and "asymmetric" have been used in reference to the actual coefficients, whereas the modifying superlatives "least" and "most" have been used in reference to the phase nonlinearity of the coefficients. In particular, asymmetric coefficients with either minimal or maximal phase nonlinearity ($\mathrm{pnl}(\mathcal{A}) > 0$) have been called, respectively, "least asymmetric" and "most asymmetric" for the complex orthogonal case with even K and for the real orthogonal case. Analogously, symmetric coefficients with minimal or maximal $\mathrm{pnl}(\mathcal{A}) > 0$ have been called, respectively, "most symmetric" and "least symmetric" for the complex orthogonal case with odd K. The unmodified term "symmetric" has been used for the real biorthogonal case where symmetric coefficients with linear phase ($\mathrm{pnl}(\mathcal{A}) = 0$ and $\mathrm{pnl}(\mathcal{S}) = 0$) are possible.

Some of these families can be collected as unions. Defining another family as complex orthogonal "least nonlinear" for all K permits the union of the most symmetric for odd K with the least asymmetric for even K. Thus, DCOLN = DCOMS $\cup$ DCOLA. Similary, defining the family complex orthogonal "most nonlinear" permits the union of the least symmetric for odd K with the most asymmetric for even K. Thus, DCOMN = DCOLS $\cup$ DCOMA. In the real case, there is no need for an analogous definition since DROLA and DROMA are each defined for all K. Thus, DROLN = DROLA and DROMN = DROMA as simply a relabeling of names without any distinction in defining criteria or algorithms.

Contrast this relabeling of the same definition with the examples of the pairs DROMD and DROMA, and DCOMD and DCOMN, which have distinct defining algorithms. In fact, roots for each of DROMD and DCOMD are selected strictly by geometric criteria without an optimization search, while roots for each of DROMA and DCOMN are selected by maximizing $\mathrm{pnl}(\mathcal{A}) > 0$ over all possible combinatorial subsets of roots. However, both equivalences DROMD = DROMA and DCOMD = DCOMN for all K were experimentally observed as expected, thus providing an important consistency test of this part of the theory and implementation of the algorithms in an actual computer program.

Use of the automated algorithms results in the identification of new and interesting wavelets. As one particular example, for the DRBBR family, an analysis-synthesis pair, each with $K = 5$ vanishing moments and length $N = 10$ coefficients, but with different time-domain regularities of $\mathrm{tdr}(\mathcal{A}) = 1.213$ and $\mathrm{tdr}(\mathcal{S}) = 2.321$, has been identified as the shortest of a sequence of pairs which occurs for $\{K = 1 + 4k \mid k = 1, 2, \ldots\}$. This new biorthogonal (10,10;5,5) filter pair can be compared with the well-known (9,7;4,4) pair with regularities $\mathrm{tdr}(\mathcal{A}) = 1.068$ and $\mathrm{tdr}(\mathcal{S}) = 1.701$. In the setting of image compression with symmetric biorthogonal filters, the increased regularity

of the (10,10;5,5) pair should help reduce reconstruction artifacts.

Reviewing the various filter families generated by the algorithms, some general conclusions can be made. With regard to the product filters, both $\mathcal{P}_{\mathcal{D}}(z)$ and $\mathcal{P}_{\mathcal{L}}(z)$ are suitable for both computation of roots and generation of coefficients for low degree polynomials. However, as expected for higher degree polynomials, $\mathcal{P}_{\mathcal{D}}(z)$ and $\mathcal{P}_{\mathcal{L}}(z)$ prove to be more numerically stable, respectively, for roots (Section 3.1) and coefficients (Section 3.2). Using $\mathcal{P}_{\mathcal{D}}(z)$ as the source of the roots and $\mathrm{moe}(\mathbf{A})$ as a measure of stability with tolerance set at 1×10^{-6} and $\mathbf{A}$ taken from either the DROMD or DCOMD families, then coefficients from the roots can be readily computed in a stable manner up to $\mathcal{D} = 35$ and $\mathcal{D} = 56$ corresponding to their use respectively for DROMD(72;36) and DCOMD(114;57) with $K = 36$ and $K = 57$ in these families which do not require optimizing searches.

To search root subsets for the other orthogonal families, given the order K and thus $n^{\mathrm{cq}} = \lfloor (K-1)/2 \rfloor$ complex quadruplets and $n^{\mathrm{rd}} = (K-1) \mod 2$ real duplets, there are a total of $2^{n^{\mathrm{cq}}+n^{\mathrm{rd}}-1}$ subsets for the full search ignoring complements. Denoting the partial searches with $k_{\min}$ and $k_{\max}$, there are a total of $\sum_{k=k_{\min}}^{k_{\max}} \binom{n^{\mathrm{cq}}+n^{\mathrm{rd}}}{k}$ subsets ignoring complements. DROMR was the only family observed to require $k_{\min} = 0$ and $k_{\max} = \lfloor K/4 \rfloor$, while DCOMR required $k_{\min} = \lfloor K/4 \rfloor - 2$ and $k_{\max} = \lfloor K/4 \rfloor$. But for given K, $\mathrm{tdr}(\mathcal{A})$ for all of the orthogonal families was sufficiently similar that it would not justify such an expensive optimization search for high order K. Nevertheless, other orthogonal families such as DROLU, DCOLU, and DCOLN required $k_{\min} = \lfloor K/4 \rfloor - 1$ and $k_{\max} = \lfloor K/4 \rfloor$ while DROLA required $k_{\min} = k_{\max} = \lfloor K/4 \rfloor$. (Since DROMA = DROMD and DCOMN = DCOMD, optimizing searches are not necessary for these families because they can always be computed via DROMD and DCOMD.) Given the empirical conjecture that these partial searches are sufficient, then optimizing searches for these other families up to the orders $K = 36$ and $K = 57$ mentioned above are in fact feasible on today's fast machines because for $(n^{\mathrm{cq}} = 17, n^{\mathrm{rd}} = 1)$ and $(n^{\mathrm{cq}} = 28, n^{\mathrm{rd}} = 0)$ there are respectively $\binom{18}{8} + \frac{1}{2}\binom{18}{9} = 6.8 \times 10^4$ and $\binom{28}{13} + \frac{1}{2}\binom{28}{14} = 5.8 \times 10^7$ subsets (recalling $\binom{n}{k} = \frac{1}{2}\binom{n}{n/2}$ for even n and $k = n/2$ when ignoring complements).

Since the rate-limiting step in the algorithm is the evaluation of each binomial coded subset of roots, the computational complexity is approximately $\mathcal{O}(cK\binom{n^{\mathrm{cq}}+n^{\mathrm{rd}}}{\lfloor K/4 \rfloor})$ where c is a constant determined by the type of filter characteristic evaluated during the search. Thus, combinatorial searches remain practical for Daubechies wavelets of moderate order $K \leq 36$ and even higher order $K \leq 57$ when optimized in search spaces parameterized by the order K and the binary codes of the binomial subsets for the roots obtained from spectral factorization. Even though the empirically observed $\mathrm{vmn}(\mathbf{a}_1) = K$ for all orthogonal families only for $K \leq 13$, and peak at $\mathrm{vmn}(\mathbf{a}_1) \approx 17$ for some of the families, the use of increasing $K > 17$ does serve to constrain the search space for higher order wavelets with increasing N, increasing $\mathrm{fds}(\mathbf{A})$, and whichever other desired filter characteristic. In contrast, results for methods based on angular parameterizations with lattice filter designs have so far been demonstrated only for $K \leq 3$.

Systematizing a collection of Daubechies wavelet filters with a mechanism both for generating and evaluating the filters enables the development of filter catalogues with tables of numerical

parameter estimates characterizing their properties such as those found in Tables 3–10. Providing estimates for a variety of characteristics in both time and frequency domains, rather than just the optimized characteristic, constitutes an important aspect of these tables which enhances their utility. Use of these reference catalogues as a convenient resource then enables the investigator to choose an available filter with the desired characteristics most appropriate to the research problem or development application.

References

[1] Ali N. Akansu and Richard A. Haddad. *Multiresolution Signal Decomposition Transforms, Subbands, and Wavelets*. Academic Press, San Diego, CA, 1992. 2.2.3

[2] Ali N. Akansu, Richard A. Haddad, and H. Caglar. The binomial QMF-wavelet transform for multiresolution signal decomposition. *IEEE Transactions on Signal Processing*, 41:13–19, January 1993. 1

[3] R. Ansari, C. Guillemot, and J. F. Kaiser. Wavelet construction using Lagrange halfband filters. *IEEE Transactions on Circuits and Systems*, 38(9):1116–1118, September 1991. 1, 2.1.2

[4] Albert Cohen, Ingrid Daubechies, and J. C. Feauveau. Biorthogonal bases of compactly supported wavelets. *Communications on Pure and Applied Mathematics*, 45:485–560, 1992. 1, 1

[5] Ingrid Daubechies. Orthonormal bases of compactly supported wavelets. *Communications on Pure and Applied Mathematics*, 41:909–996, 1988. 1, 1, 2.1.3, 2.4.2

[6] Ingrid Daubechies. *Ten Lectures on Wavelets*. Number 61 in CBMS-NSF Series in Applied Mathematics. Society for Industrial and Applied Mathematics, Philadelphia, PA, 1992. 1, 1, 2.1.3, 2.1.3, 2.2.3, 2.3.3, 2.3.3

[7] Ingrid Daubechies. Orthonormal bases of compactly supported wavelets: II. variations on a theme. *SIAM Journal on Mathematical Analysis*, 24(2):499–519, March 1993. 1, 1

[8] Gilles Deslauriers and Serge Dubuc. Interpolation through an iterative scheme. *Constructive Approximation*, 5:49–68, 1989. 2.1.2

[9] Christian Dorize and Lars F. Villemoes. Optimizing time-frequency resolution of orthonormal wavelets. In *Proceedings of the IEEE International Conference on Acoustics, Speech, and Signal Processing*, volume 3, pages 2029–2032, May 1991. 1

[10] Miloš I. Doroslovački. Diminishing the asymmetry of Daubechies' wavelets. In Moeness G. Amin, editor, *Proceedings of the IEEE-SP International Symposium on Time-Frequency and Time-Scale Analysis*, pages 5–8, October 1994. 1

[11] Miloš I. Doroslovački. On the least asymmetric wavelets. *IEEE Transactions on Signal Processing*, 46(4):1125–1130, April 1998. 1

[12] A. Edrei. Sur les déterminants récurrents et les singularités d'une fonction donnée par son developpement de Taylor. *Composito Math.*, 7:20–88, 1939. 2.2.1

[13] D. Esteban and C. Galand. Application of quadrature mirror filters to split band voice coding schemes. *Proceedings of the IEEE International Conference on Acoustics, Speech, and Signal Processing*, pages 191–195, May 1977. 2.2.3

[14] N. J. Fliege. *Multirate Digital Signal Processing: Multirate Systems, Filter Banks, Wavelets.* John Wiley & Sons, Chichester, England, 1994. 2.2.3

[15] Tim N. T. Goodman, Charles A. Micchelli, Giuseppe Rodriguez, and Sebastiano Seatzu. Spectral factorization of Laurent polynomials. *Advances in Computational Mathematics*, 1997. 1, 2.1.1, 2.1.2, 2.1.3, 2.1.3, 2.3.1

[16] Cormac Herley. Exact interpolation and iterative subdivision schemes. *IEEE Transactions on Signal Processing*, 43(6):1348–1359, June 1995. 2.1.2

[17] Nicholar J. Higham. *Accuracy and Stability of Numerical Algorithms.* Society for Industrial and Applied Mathematics, Philadelphia, PA, 1996. 2.2.1

[18] Markus Lang and Bernhard-Christian Frenzel. Polynomial root finding. 1(10):141–143, October 1994. 2.2.1

[19] Wayne M. Lawton. Necessary and sufficient conditions for constructing orthonormal wavelet bases. *J. Math. Phys.*, 32(1):57–61, January 1991. 1

[20] Wayne M. Lawton. Applications of complex valued wavelet transforms to subband decompositions. *IEEE Transactions on Signal Processing*, 41(12):3566–3568, December 1993. 1

[21] F. Leja. Sur certaines suits liées aux ensembles plans et leur application à la representation conforme. *Ann. Polon. Math.*, 4:8–13, 1957. 2.2.1

[22] Jean-Marc Lina and Michel Mayrand. Parameterizations for Daubechies wavelets. *Physical Review E*, 48(6):R4160–4163, December 1993. 1

[23] Jean-Marc Lina and Michel Mayrand. Complex Daubechies wavelets. *Applied and Computational Harmonic Analysis*, 2(3):219–229, July 1995. 1

[24] Aleksei Ivanovich Markushevich. *Theory of Functions of a Complex Variable.* Chelsea Publishing Company, New York, second edition, 1977. translated by Richard A. Silverman. 2.1.3

[25] The MathWorks, Inc., Natick, MA. *MATLAB The Language of Technical Computing: MATLAB 5.1 New Features*, May 1997. 2.5

[26] Joel M. Morris and Vinod Akunuri. Minimum duration orthonormal wavelets. *Optical Engineering*, 35(7):2079–2087, July 1996. 1

[27] Joel M. Morris and Hui Xie. Minimum duration-bandwidth discrete-time wavelets. *Optical Engineering*, 35(7):2075–2078, July 1996. 1

[28] Athanasios Papoulis. *Signal Analysis.* McGraw-Hill, Inc., New York, NY, 1977. 1

[29] David Pollen. $SU_I F[z, 1/z]$ for F a subfield of C. *Journal of the American Mathematical Society*, 3(3):611–624, July 1990. 1

[30] William H. Press, Saul A. Teukolsky, William T. Vetterling, and Brian P. Flannery. *Numerical Recipes in C: The Art of Scientific Computing.* Cambridge University Press, second edition, 1992. 1

[31] Lothar Reichel. Newton interpolation at Leja points. *BIT*, 30:332–346, 1990. 2.2.1

[32] Lothar Reichel. The application of Leja points to Richardson iteration and polynomial preconditioning. *Linear Algebra and Its Applications*, 154–156:389–414, 1991. 2.2.1

[33] Edward M. Reingold, Jurg Nievergelt, and Narsingh Deo. *Combinatorial Algorithms: Theory and Practice*. Prentice-Hall, Inc., Englewood Cliffs, NJ, 1977. 6

[34] Peter Rieder, Jürgen Götze, Josef A. Nossek, and C. Sidney Burrus. Parameterization of orthogonal wavelet transforms and their implementation. *IEEE Transactions on Circuits and Systems II. Analog and Digital Signal Processing*, 45(2):217–226, February 1998. 1

[35] Frigyes Riesz and Béla Sz.-Nagy. *Functional Analysis*. Dover Publications, Inc., Mineola, NY, 1990. first published 1955; translated from the second French edition by Leo F. Boron. 1

[36] Jianhong Shen and Gilbert Strang. The zeros of the daubechies polynomials. *Proceedings of the American Mathematical Society*, 124(12):3819–3833, 1996. 1, 2.1.3, 2.1.3

[37] Mark J. Shensa. The discrete wavelet transform: Wedding the à trous and Mallat algorithms. *IEEE Transactions on Signal Processing*, 40(10):2464–2482, October 1992. 1, 2.1.2, 2.1.2

[38] B. G. Sherlock and D. M. Monro. On the space of orthonormal wavelets. *IEEE Transactions on Signal Processing*, 46(6):1716–1720, June 1998. 1, 1

[39] Mark J. T. Smith and Thomas P. Barnwell III. A procedure for designing exact reconstruction filter banks for tree-structured subband coders. *Proceedings of the IEEE International Conference on Acoustics, Speech, and Signal Processing*, pages 27.1.1–27.1.4, March 1984. 2.2.3

[40] Gilbert Strang. The optimal coefficients in Daubechies wavelets. *Physica D*, 60:239–244, 1992. 1

[41] Gilbert Strang and Truong Nguyen. *Wavelets and Filter banks*. Wellesley-Cambridge Press, 1996. 2.2.3

[42] Carl Taswell. *WAVBOX Software Library and Reference Manual*. Computational Toolsmiths, www.wavbox.com, 1993–98. 2.5

[43] Carl Taswell. Algorithms for the generation of Daubechies orthogonal least asymmetric wavelets and the computation of their Holder regularity. Technical report, Scientific Computing and Computational Mathematics, Stanford University, August 1995. 1

[44] Carl Taswell. Specifications and standards for reproducibility of wavelet transforms. In *Proceedings of the International Conference on Signal Processing Applications and Technology*, pages 1923–1927. Miller Freeman, October 1996. 1

[45] Carl Taswell. Computational algorithms for Daubechies least-asymmetric, symmetric, and most-symmetric wavelets. In *Proceedings of the International Conference on Signal Processing Applications and Technology*, pages 1834–1838. Miller Freeman, September 1997. 1, 1, 1, 2.3.3, 2.4.2

[46] Carl Taswell. *The Systematized Collection of Wavelet Filters Computable by Spectral Factorization of the Daubechies Polynomial*. Computational Toolsmiths, www.toolsmiths.com, 1997. 2.2.1, 3.2, 3.4, 3.5

[47] Carl Taswell. Correction for the Sherlock-Monro algorithm for generating the space of real orthonormal wavelets. Technical Report CT-1998-05, Computational Toolsmiths, www.toolsmiths.com, June 1998. 1

[48] Carl Taswell. Empirical tests for the evaluation of multirate filter bank parameters. Technical Report CT-1998-02, Computational Toolsmiths, www.toolsmiths.com, March 1998. 1, 2.3.4, 7, 3.3, 3.5

[49] Carl Taswell. Reproducibility standards for wavelet transform algorithms. Technical Report CT-1998-01, Computational Toolsmiths, www.toolsmiths.com, March 1998. 1

[50] Carl Taswell. A spectral-factorization combinatorial-search algorithm unifying the systematized collection of Daubechies wavelets. In *Proceedings of the IAAMSAD International Conference on Systems, Signals, Control, and Computers*, September 1998. Invited Paper and Session Keynote Lecture, Paper #323, in press. 1, 2.4.2, 2.4.2

[51] Nico M. Temme. Asymptotics and numerics of zeros of polynomials that are related to Daubechies wavelets. *Applied and Computational Harmonic Analysis*, 4(4):414–428, October 1997. 1, 1, 2.3.1

[52] P. P. Vaidyanathan. *Multirate Systems and Filter Banks*. Prentice Hall Signal Processing Series. P T R Prentice-Hall, Inc., Englewood Cliffs, NJ, 1993. 2.2.3

[53] S. H. Wang, Ahmed H. Tewfik, and Hehong Zou. Correction to 'parametrization of compactly supported orthonormal wavelets'. *IEEE Transactions on Signal Processing*, 42(1):208–209, January 1994. 1

[54] Hehong Zou and Ahmed H. Tewfik. Parametrization of compactly supported orthonormal wavelets. *IEEE Transactions on Signal Processing*, 41(3):1428–1431, March 1993. 1, 1

Table 1: List of Named Filters for Systematized Collection of Daubechies Wavelets

Name for Product $\mathcal{P}(z)$	Label
Lagrange Real Nonorthogonal Symmetric Interpolating	LRNSI$(N; K; d)$
Daubechies Real Nonorthogonal Symmetric Interpolating	DRNSI$(N; K; d)$

Name for Analysis and Synthesis Factors $\mathcal{A}(z)$ and $\mathcal{S}(z)$	Label
Daubechies Real Biorthogonal Symmetric Spline	DRBSS$(N_a, N_s; K_a, K_s)$
Daubechies Real Biorthogonal Most Disjoint	DRBMD$(N_a, N_s; K_a, K_s)$
Daubechies Real Biorthogonal Least Regular	DRBLR$(N_a, N_s; K_a, K_s)$
Daubechies Real Biorthogonal Most Regular	DRBMR$(N_a, N_s; K_a, K_s)$
Daubechies Real Biorthogonal Least Selective	DRBLS$(N_a, N_s; K_a, K_s)$
Daubechies Real Biorthogonal Most Selective	DRBMS$(N_a, N_s; K_a, K_s)$
Daubechies Real Biorthogonal Least Uncertain	DRBLU$(N_a, N_s; K_a, K_s)$
Daubechies Real Biorthogonal Most Uncertain	DRBMU$(N_a, N_s; K_a, K_s)$
Daubechies Real Biorthogonal Balanced Regular	DRBBR$(N_a, N_s; K_a, K_s)$
Daubechies Real Biorthogonal Balanced Selective	DRBBS$(N_a, N_s; K_a, K_s)$
Daubechies Real Biorthogonal Balanced Uncertain	DRBBU$(N_a, N_s; K_a, K_s)$

Name for Square Root Analysis Factor $\mathcal{A}(z)$	Label
Daubechies Real Orthogonal Most Disjoint	DROMD$(N; K)$
Daubechies Complex Orthogonal Most Disjoint	DCOMD$(N; K)$
Daubechies Real Orthogonal Least Uncertain	DROLU$(N; K)$
Daubechies Complex Orthogonal Least Uncertain	DCOLU$(N; K)$
Daubechies Real Orthogonal Most Regular	DROMR$(N; K)$
Daubechies Complex Orthogonal Most Regular	DCOMR$(N; K)$
Daubechies Real Orthogonal Least Asymmetric	DROLA$(N; K)$
Daubechies Complex Orthogonal Least Asymmetric	DCOLA$(N; K)$
Daubechies Real Orthogonal Most Asymmetric	DROMA$(N; K)$
Daubechies Complex Orthogonal Most Asymmetric	DCOMA$(N; K)$
Daubechies Complex Orthogonal Least Symmetric	DCOLS$(N; K)$
Daubechies Complex Orthogonal Most Symmetric	DCOMS$(N; K)$
Daubechies Complex Orthogonal Least Nonlinear	DCOLN$(N; K)$
Daubechies Complex Orthogonal Most Nonlinear	DCOMN$(N; K)$

Filters have length N coefficients and K roots at $z = -1$. Interpolating filters are exact for polynomials of regular degree d. All biorthogonal filters are symmetric. All biorthogonal filters except DRBSS have balanced length.

Table 2: Summary of Filter Designs for Systematized Collection of Daubechies Wavelets

Nonorthogonal $\mathcal{P}(z)$	Construction	Constraint	
LRNSI$(N;K;d)$	$\mathcal{P}_{\mathcal{L}}(z)$ coefs	$\mathcal{L} \geq 1$	
DRNSI$(N;K;d)$	via $\mathcal{Q}_{\mathcal{D}}(z)$ roots	$\mathcal{D} \geq 0$	
Biorthogonal $\mathcal{A}(z)$, $\mathcal{S}(z)$	**Factorization**	**Constraint**	**Optimization**
DRBSS$(N_a,N_s;K_a,K_s)$	$\{z_j \neq -1\}$ to $\mathcal{A}(z)$	even (K_a+K_s)	none
DRBMS$(N_a,N_s;K_a,K_s)$	conj recip quads	even (K_a+K_s)	$\max \mathrm{fds}(\mathcal{A})$
DRBLU$(N_a,N_s;K_a,K_s)$	conj recip quads	even (K_a+K_s)	$\min \mathrm{tfu}(\mathcal{A})$
DRBMR$(N_a,N_s;K_a,K_s)$	conj recip quads	even (K_a+K_s)	$\max \mathrm{tdr}(\mathcal{A})$
DRBBR$(N_a,N_s;K_a,K_s)$	conj recip quads	even (K_a+K_s)	$\max B(\mathrm{tdr}(\cdot),\mathcal{A},\mathcal{S})$
Orthogonal $\mathcal{A}(z)$	**Factorization**	**Constraint**	**Optimization**
DROMD$(N;K)$	$\{z_j = r_j e^{i\alpha_j} \mid r_j < 1\}$	$K \geq 1$	none
DCOMD$(N;K)$	$\{(z_j, z_j^{-1}) \mid r_j < 1, \alpha_j \geq 0\}$	$K \geq 3$	none
DROLU$(N;K)$	quads $\rightarrow$ conj dups	$K \geq 1$	$\min \mathrm{tfu}(\mathcal{A})$
DCOLU$(N;K)$	quads $\rightarrow$ recip dups	$K \geq 3$	$\min \mathrm{tfu}(\mathcal{A})$
DROMR$(N;K)$	quads $\rightarrow$ conj dups	$K \geq 1$	$\max \mathrm{tdr}(\mathcal{A})$
DCOMR$(N;K)$	quads $\rightarrow$ recip dups	$K \geq 3$	$\max \mathrm{tdr}(\mathcal{A})$
DROLA$(N;K)$	quads $\rightarrow$ conj dups	$K \geq 1$	$\min \mathrm{pnl}(\mathcal{A})$
DCOLA$(N;K)$	quads $\rightarrow$ recip dups	even $K \geq 4$	$\min \mathrm{pnl}(\mathcal{A})$
DROMA$(N;K)$	quads $\rightarrow$ conj dups	$K \geq 1$	$\max \mathrm{pnl}(\mathcal{A})$
DCOMA$(N;K)$	quads $\rightarrow$ recip dups	even $K \geq 4$	$\max \mathrm{pnl}(\mathcal{A})$
DCOLS$(N;K)$	quads $\rightarrow$ recip dups	odd $K \geq 3$	$\max \mathrm{pnl}(\mathcal{A})$
DCOMS$(N;K)$	quads $\rightarrow$ recip dups	odd $K \geq 3$	$\min \mathrm{pnl}(\mathcal{A})$
DCOLN$(N;K)$	quads $\rightarrow$ recip dups	$K \geq 3$	$\min \mathrm{pnl}(\mathcal{A})$
DCOMN$(N;K)$	quads $\rightarrow$ recip dups	$K \geq 3$	$\max \mathrm{pnl}(\mathcal{A})$

Product filter $\mathcal{P}(z)$ is split into spectral factors for analysis filter $\mathcal{A}(z)$ and synthesis filter $\mathcal{S}(z)$. Names are abbreviated with first character L or D for Lagrange or Daubechies, second character R or C for Real or Complex, and third character N, B, or O for nonorthogonal, biorthogonal, or orthogonal. Complex conjugate reciprocal quadruplets are split into conjugate duplets or reciprocal duplets. Real reciprocal duplets are split into real singlets but have been omitted from the table. See Section 2.4 and especially Sections 2.4.1 and 2.4.2 for further explanation of factorization rules and selection criteria, respectively.

Table 3: Biorthogonal Scalets Time-Domain Regularity tdr($\mathcal{A}$) and tdr($\mathcal{S}$).

K	DRBMR		DRBLU		DRBBR		DRBMS		DRBSS	
	$\mathcal{A}$	$\mathcal{S}$	$\mathcal{A}$	$\mathcal{S}$	$\mathcal{A}$	$\mathcal{S}$	$\mathcal{A}$	$\mathcal{S}$	$\mathcal{A}$	$\mathcal{S}$
1	0.000	0.000	0.000	0.000	0.000	0.000	0.000	0.000	0.000	0.000
2	-0.000	1.000	-0.000	1.000	-0.000	1.000	-0.000	1.000	-0.000	1.000
3	-0.170	2.000	-0.170	2.000	-0.170	2.000	-0.170	2.000	-0.170	2.000
4	1.068	1.701	1.068	1.701	1.068	1.701	1.068	1.701	-0.449	3.000
5	2.321	1.213	2.321	1.213	1.213	2.321	2.321	1.213	-0.806	4.000
6	1.899	2.324	1.899	2.324	1.899	2.324	1.899	2.324	-1.223	5.000
7	1.881	2.960	1.881	2.960	1.881	2.960	1.881	2.960	-1.683	6.000
8	3.215	2.270	3.215	2.270	2.596	2.890	2.596	2.890	-2.171	7.000
9	3.545	2.526	3.545	2.526	2.526	3.545	3.545	2.526	-2.677	8.000
10	3.919	2.693	3.919	2.693	3.206	3.407	2.831	3.783	-3.195	9.000
11	3.867	3.252	3.444	3.677	3.444	3.677	2.710	4.412	-3.720	10.000
12	5.215	2.430	4.506	3.140	3.760	3.887	3.303	4.345	-4.252	11.000
13	5.630	2.513	5.630	2.513	4.038	4.105	4.397	3.746	-4.788	12.000
14	5.852	2.768	4.853	3.769	4.280	4.342	3.783	4.839	-5.327	13.000
15	5.786	3.301	5.126	3.962	4.618	4.470	3.625	5.465	-5.870	14.000
16	7.140	2.419	5.530	4.030	4.778	4.782	4.400	5.161	-6.415	15.000
17	7.602	2.419	6.451	3.570	5.004	5.018	4.840	5.182	-6.962	16.000
18	7.751	2.725	7.751	2.725	5.262	5.215	4.923	5.554	-7.511	17.000
19	7.682	3.245	7.682	3.245	5.469	5.459	4.536	6.393	-8.062	18.000
20	9.040	2.339	9.040	2.339	5.660	5.720	5.296	6.084	-8.614	19.000
21	9.532	2.296	9.532	2.296	5.883	5.945	6.123	5.705	-9.168	20.000
22	9.638	2.635	9.638	2.635	6.133	6.141	5.799	6.475	-9.723	21.000
23	9.570	3.148	9.570	3.148	6.362	6.357	5.438	7.280	-10.279	22.000
24	10.930	2.232	10.930	2.232	6.565	6.597	6.202	6.960	-10.837	23.000
med	5.423	2.424	4.679	2.581	3.899	3.996	3.585	4.378	-4.520	11.500

Table 4: Orthogonal Scalets Time-Domain Regularity tdr($\mathcal{A}$).

K	DCOMR	DROMR	DCOMN	DROLU	DCOLU	DCOLN	DROMA	DROLA
1	0.000	0.000	0.000	0.000	0.000	0.000	0.000	0.000
2	0.550	0.550	0.550	0.550	0.550	0.550	0.550	0.550
3	1.000	1.088	1.000	1.088	1.000	1.000	1.088	1.088
4	1.453	1.618	1.453	1.403	1.453	1.453	1.618	1.403
5	1.828	1.969	1.828	1.776	1.789	1.789	1.969	1.776
6	2.210	2.244	2.210	2.122	2.155	2.155	2.189	2.122
7	2.537	2.579	2.537	2.485	2.449	2.449	2.460	2.468
8	2.870	2.849	2.870	2.750	2.768	2.768	2.761	2.750
9	3.161	3.123	3.161	3.039	3.039	3.039	3.074	3.039
10	3.411	3.381	3.396	3.313	3.325	3.325	3.381	3.311
11	3.638	3.626	3.613	3.588	3.576	3.574	3.603	3.579
12	3.876	3.866	3.853	3.827	3.836	3.834	3.833	3.826
13	4.106	4.101	4.081	4.098	4.074	4.075	4.073	4.072
14	4.337	4.334	4.320	4.313	4.318	4.316	4.317	4.312
15	4.565	4.563	4.549	4.552	4.549	4.549	4.558	4.550
16	4.793	4.792	4.784	4.789	4.783	4.784	4.791	4.781
17	5.019	5.019	5.012	5.016	5.011	5.011	5.014	5.011
18	5.245	5.244	5.241	5.243	5.240	5.240	5.239	5.239
19	5.469	5.469	5.467	5.466	5.465	5.465	5.465	5.465
20	5.693	5.693	5.693	5.692	5.691	5.691	5.691	5.690
21	5.916	5.916	5.916	5.915	5.914	5.914	5.916	5.914
22	6.139	6.139	6.138	6.138	6.137	6.137	6.138	6.137
23	6.360	6.360	6.360	6.360	6.359	6.359	6.360	6.359
24	6.582	6.582	6.581	6.582	6.581	6.581	6.581	6.581
med	3.991	3.984	3.967	3.963	3.955	3.954	3.953	3.949

Table 5: Biorthogonal Scalets Time-Frequency Uncertainty tfu($\mathbf{a}_0$) and tfu($\mathbf{s}_0$).

K	DRBSS		DRBMS		DRBBR		DRBMR		DRBLU	
	$\mathbf{a}_0$	$\mathbf{s}_0$	$\mathbf{a}_0$	$\mathbf{s}_0$	$\mathbf{a}_0$	$\mathbf{s}_0$	$\mathbf{a}_0$	$\mathbf{s}_0$	$\mathbf{a}_0$	$\mathbf{s}_0$
1	0.568	0.568	0.568	0.568	0.568	0.568	0.568	0.568	0.568	0.568
2	0.703	0.513	0.703	0.513	0.703	0.513	0.703	0.513	0.703	0.513
3	0.973	0.505	0.973	0.505	0.973	0.505	0.973	0.505	0.973	0.505
4	1.322	0.503	0.682	0.608	0.682	0.608	0.682	0.608	0.682	0.608
5	1.714	0.502	0.551	0.888	0.888	0.551	0.551	0.888	0.551	0.888
6	2.119	0.501	0.674	0.718	0.674	0.718	0.674	0.718	0.674	0.718
7	2.516	0.501	0.801	0.774	0.801	0.774	0.801	0.774	0.801	0.774
8	2.894	0.501	0.667	0.820	0.667	0.820	0.626	1.134	0.626	1.134
9	3.248	0.501	0.567	1.054	1.054	0.567	0.567	1.054	0.567	1.054
10	3.579	0.500	0.771	0.761	0.663	0.914	0.611	1.321	0.611	1.321
11	3.890	0.500	0.891	0.757	0.709	1.167	0.719	1.390	0.709	1.167
12	4.183	0.500	0.805	0.793	0.659	1.000	0.631	1.797	0.593	1.475
13	4.461	0.500	0.631	1.111	0.992	0.731	0.548	1.855	0.548	1.855
14	4.725	0.500	0.826	0.829	0.656	1.080	0.603	1.992	0.576	1.529
15	4.978	0.500	0.916	0.818	0.654	1.472	0.659	2.023	0.649	1.767
16	5.221	0.500	0.788	0.915	0.653	1.154	0.577	2.374	0.568	1.735
17	5.455	0.500	1.138	0.713	1.075	0.779	0.540	2.510	0.532	2.067
18	5.681	0.500	0.780	0.976	0.651	1.225	0.556	2.554	0.556	2.554
19	5.900	0.500	0.924	0.890	0.623	1.649	0.574	2.553	0.574	2.553
20	6.112	0.500	0.825	0.970	0.714	1.141	0.532	2.847	0.532	2.847
21	6.318	0.500	0.728	1.220	0.854	1.058	0.519	3.011	0.519	3.011
22	6.518	0.500	0.818	1.023	0.687	1.645	0.522	3.012	0.522	3.012
23	6.713	0.500	0.928	0.964	0.693	1.510	0.527	2.995	0.527	2.995
24	6.903	0.500	0.847	1.032	1.159	1.120	0.512	3.251	0.512	3.251
med	4.322	0.500	0.795	0.825	0.690	0.957	0.576	1.826	0.571	1.502

Table 6: Orthogonal Scalets Time-Frequency Uncertainty tfu($\mathbf{a}_0$).

K	DCOMN	DCOMR	DROMA	DROMR	DCOLN	DCOLU	DROLA	DROLU
1	0.568	0.568	0.568	0.568	0.568	0.568	0.568	0.568
2	0.592	0.592	0.592	0.592	0.592	0.592	0.592	0.592
3	0.680	0.680	0.669	0.669	0.680	0.680	0.669	0.669
4	0.829	0.829	0.755	0.755	0.829	0.829	0.635	0.635
5	1.054	1.054	0.843	0.843	0.776	0.776	0.718	0.718
6	1.270	1.270	0.931	0.734	0.802	0.802	0.694	0.694
7	1.539	1.539	1.019	1.036	0.743	0.743	0.766	0.713
8	1.785	1.785	1.106	0.778	0.796	0.796	0.748	0.748
9	2.070	2.070	1.192	0.838	0.785	0.785	0.795	0.795
10	2.332	1.944	1.278	1.278	0.835	0.835	0.795	0.765
11	2.625	1.915	1.363	1.053	0.836	0.816	0.915	0.779
12	2.896	1.879	1.447	0.911	0.903	0.869	0.838	0.800
13	3.194	1.654	1.530	0.910	0.896	0.850	0.853	0.847
14	3.471	1.741	1.613	1.228	0.923	0.894	0.853	0.830
15	3.771	1.590	1.696	1.062	0.885	0.875	0.962	0.841
16	4.053	1.888	1.778	0.961	0.973	0.917	0.882	0.853
17	4.355	1.575	1.859	0.923	0.898	0.894	0.923	0.877
18	4.640	1.556	1.940	1.604	0.998	0.938	0.909	0.873
19	4.943	1.898	2.021	1.147	0.916	0.916	1.017	0.879
20	5.231	1.761	2.101	1.591	0.980	0.958	0.909	0.895
21	5.535	1.587	2.181	0.969	0.945	0.938	0.951	0.912
22	5.825	1.525	2.261	1.470	0.999	0.978	0.929	0.915
23	6.130	1.678	2.340	1.108	0.970	0.959	1.093	0.921
24	6.422	1.511	2.420	2.774	1.025	1.002	0.950	0.934
med	3.045	1.589	1.488	0.965	0.890	0.859	0.853	0.815

Table 7: Biorthogonal Scalets Frequency-Domain Selectivity fds($\mathbf{a}_0$) and fds($\mathbf{s}_0$).

K	DRBMS		DRBBR		DRBLU		DRBMR		DRBSS	
	$\mathbf{a}_0$	$\mathbf{s}_0$	$\mathbf{a}_0$	$\mathbf{s}_0$	$\mathbf{a}_0$	$\mathbf{s}_0$	$\mathbf{a}_0$	$\mathbf{s}_0$	$\mathbf{a}_0$	$\mathbf{s}_0$
1	0.528	0.528	0.528	0.528	0.528	0.528	0.528	0.528	0.528	0.528
2	0.501	0.637	0.501	0.637	0.501	0.637	0.501	0.637	0.501	0.637
3	0.206	0.651	0.206	0.651	0.206	0.651	0.206	0.651	0.206	0.651
4	0.695	0.760	0.695	0.760	0.695	0.760	0.695	0.760	-0.186	0.636
5	0.634	0.487	0.487	0.634	0.634	0.487	0.634	0.487	-0.717	0.611
6	0.712	0.769	0.712	0.769	0.712	0.769	0.712	0.769	-1.439	0.583
7	0.649	0.729	0.649	0.729	0.649	0.729	0.649	0.729	-2.433	0.555
8	0.720	0.755	0.720	0.755	0.566	0.287	0.566	0.287	-3.812	0.530
9	0.713	0.607	0.607	0.713	0.713	0.607	0.713	0.607	-5.739	0.506
10	0.786	0.814	0.725	0.737	0.557	0.145	0.557	0.145	-8.450	0.484
11	0.772	0.836	0.584	0.426	0.584	0.426	0.498	-0.023	-12.288	0.465
12	0.783	0.809	0.728	0.720	0.559	0.073	0.436	-1.019	-17.751	0.447
13	0.790	0.759	0.793	0.771	0.521	-0.513	0.521	-0.513	-25.568	0.431
14	0.792	0.817	0.730	0.704	0.610	0.247	0.430	-1.322	-36.801	0.417
15	0.825	0.876	0.572	0.233	0.482	-0.410	0.387	-1.730	-53.010	0.403
16	0.838	0.871	0.732	0.690	0.573	0.014	0.348	-3.830	-76.482	0.391
17	0.810	0.806	0.793	0.767	0.574	-0.275	0.402	-2.960	-110.586	0.380
18	0.835	0.863	0.733	0.677	0.346	-4.499	0.346	-4.499	-160.286	0.370
19	0.844	0.889	0.621	0.325	0.316	-5.421	0.316	-5.421	-232.913	0.360
20	0.853	0.882	0.729	0.688	0.291	-10.016	0.291	-10.016	-339.306	0.351
21	0.826	0.821	0.788	0.806	0.328	-8.428	0.328	-8.428	-495.518	0.343
22	0.855	0.880	0.744	0.691	0.291	-11.529	0.291	-11.529	-725.358	0.335
23	0.851	0.892	0.580	0.241	0.269	-13.599	0.269	-13.599	-1064.177	0.328
24	0.864	0.890	0.616	0.442	0.253	-23.922	0.253	-23.922	-1564.530	0.321
med	0.788	0.812	0.703	0.691	0.542	0.109	0.433	-0.766	-21.660	0.439

Table 8: Orthogonal Scalets Phase NonLinearity pnl($\mathcal{A}$).

K	DCOMN	DROMA	DCOMR	DROMR	DROLU	DCOLU	DCOLN	DROLA
1	0.000	0.000	0.000	0.000	0.000	0.000	0.000	0.000
2	1.081	1.081	1.081	1.081	1.081	1.081	1.081	1.081
3	2.670	2.300	2.670	2.300	2.300	2.670	2.670	2.300
4	4.607	3.578	4.119	3.578	0.914	4.119	4.119	0.914
5	6.810	4.889	6.810	4.889	0.564	3.381	3.381	0.564
6	8.974	6.220	8.974	3.359	0.849	2.863	2.863	0.849
7	11.295	7.566	11.295	3.555	2.237	1.364	1.364	1.841
8	13.605	8.922	13.216	3.697	0.863	1.755	1.313	0.863
9	15.931	10.287	15.931	4.304	0.590	0.619	0.619	0.590
10	18.328	11.659	14.791	11.659	0.988	1.341	1.341	0.897
11	20.648	13.036	14.043	3.562	2.184	1.077	0.998	1.864
12	23.105	14.417	13.495	4.106	1.020	1.876	1.754	0.937
13	25.418	15.802	11.334	4.181	4.532	1.552	0.926	0.322
14	27.915	17.190	12.445	11.844	1.028	1.769	1.568	0.860
15	30.222	18.581	10.539	3.492	2.144	0.949	0.756	1.795
16	32.751	19.974	13.772	4.172	3.600	1.832	1.380	0.861
17	35.053	21.370	9.982	4.345	4.830	1.220	0.538	0.335
18	37.606	22.767	8.076	19.597	3.530	1.494	1.392	0.868
19	39.903	24.166	14.231	12.007	2.291	0.605	0.605	1.782
20	42.474	25.567	11.997	19.813	3.525	1.566	1.405	0.847
21	44.767	26.969	5.001	4.464	4.896	1.025	0.305	0.304
22	47.355	28.372	6.120	4.968	3.529	1.536	1.402	0.854
23	49.644	29.776	11.116	12.160	2.286	0.688	0.511	1.795
24	52.244	31.182	6.254	27.242	3.674	1.451	1.408	0.849
med	24.261	15.109	10.827	4.243	2.210	1.472	1.352	0.862

Table 9: Biorthogonal Wavelets Vanishing Moments Numbers vmn($\mathbf{a}_1$) and vmn($\mathbf{s}_1$).

K	DRBMS		DRBBR		DRBLU		DRBMR		DRBSS	
	$\mathbf{a}_1$	$\mathbf{s}_1$	$\mathbf{a}_1$	$\mathbf{s}_1$	$\mathbf{a}_1$	$\mathbf{s}_1$	$\mathbf{a}_1$	$\mathbf{s}_1$	$\mathbf{a}_1$	$\mathbf{s}_1$
1	1	1	1	1	1	1	1	1	1	1
2	2	2	2	2	2	2	2	2	2	2
3	3	3	3	3	3	3	3	3	3	3
4	4	4	4	4	4	4	4	4	4	4
5	5	5	5	5	5	5	5	5	5	5
6	6	6	6	6	6	6	6	6	6	6
7	7	7	7	7	7	7	7	7	7	7
8	8	8	8	8	8	8	8	8	8	8
9	9	9	9	9	9	9	9	9	9	9
10	10	10	10	10	10	10	10	10	10	10
11	11	11	11	11	11	11	11	11	11	11
12	12	12	12	12	12	12	12	12	12	12
13	13	13	13	13	13	13	13	13	13	13
14	14	14	14	14	14	14	14	14	14	14
15	15	15	15	15	15	15	15	15	15	11
16	16	16	16	16	16	16	16	16	16	12
17	17	16	17	17	17	17	16	17	14	10
18	17	16	16	16	15	17	15	17	14	10
19	17	15	16	15	16	16	16	16	14	10
20	16	15	15	15	14	16	14	16	14	10
21	15	15	15	15	13	16	13	16	12	9
22	15	14	15	14	13	16	13	16	12	9
23	15	13	14	15	13	15	13	15	12	8
24	14	13	14	13	12	15	12	15	11	8
med	13	13	13	13	12	13	12	13	12	9

Table 10: Orthogonal Wavelets Vanishing Moments Numbers vmn($\mathbf{a}_1$).

K	DROLA	DCOLN	DROLU	DCOLU	DCOMR	DROMR	DCOMN	DROMA
1	1	1	1	1	1	1	1	1
2	2	2	2	2	2	2	2	2
3	3	3	3	3	3	3	3	3
4	4	4	4	4	4	4	4	4
5	5	5	5	5	5	5	5	5
6	6	6	6	6	6	6	6	6
7	7	7	7	7	7	7	7	7
8	8	8	8	8	8	8	8	8
9	9	9	9	9	9	9	9	9
10	10	10	10	10	10	10	10	10
11	11	11	11	11	11	11	11	11
12	12	12	12	12	12	12	12	12
13	13	13	13	13	13	13	13	13
14	14	14	14	14	14	13	14	13
15	15	15	15	15	15	15	14	12
16	16	16	16	16	16	15	13	12
17	17	16	16	17	17	16	12	10
18	16	16	16	16	17	11	11	10
19	15	15	15	15	14	13	11	10
20	15	15	14	15	16	10	11	9
21	15	16	14	15	14	14	11	9
22	15	13	13	14	16	14	9	9
23	13	13	13	13	16	11	10	8
24	14	13	13	13	14	8	9	7
med	13	13	13	13	13	11	10	9

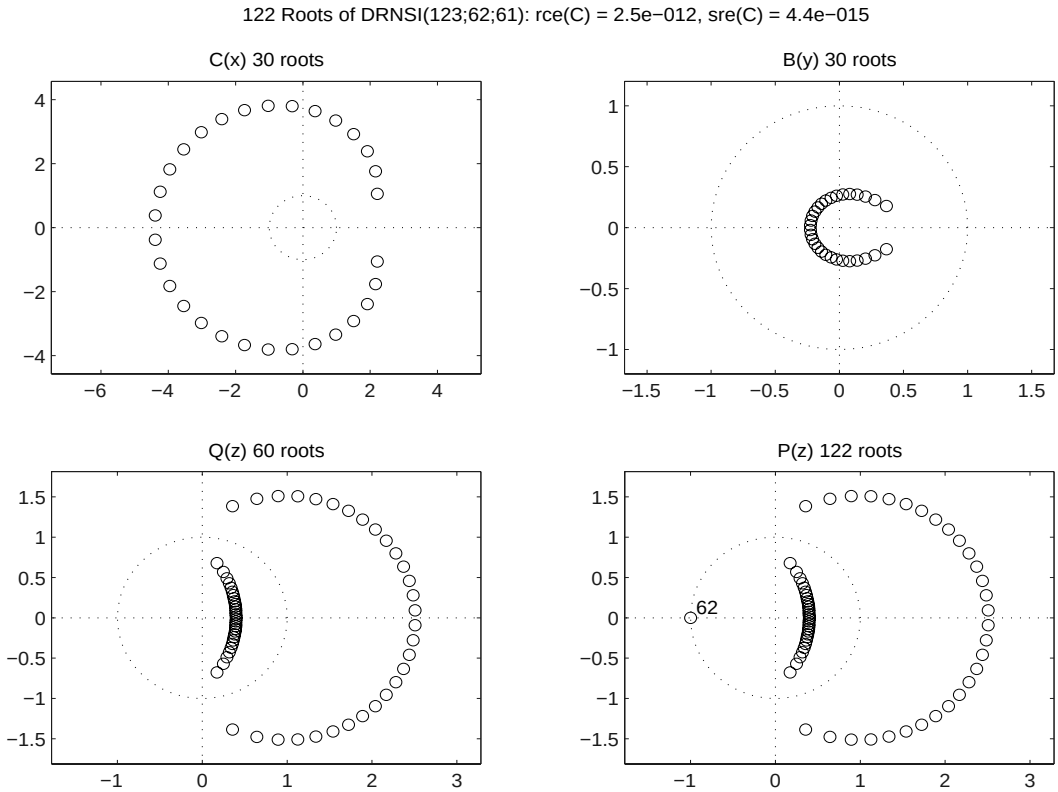

Figure 1: Related Forms of Daubechies Polynomial $\mathcal{P}_{\mathcal{D}}(z)$ for $\mathcal{D} = 30$.

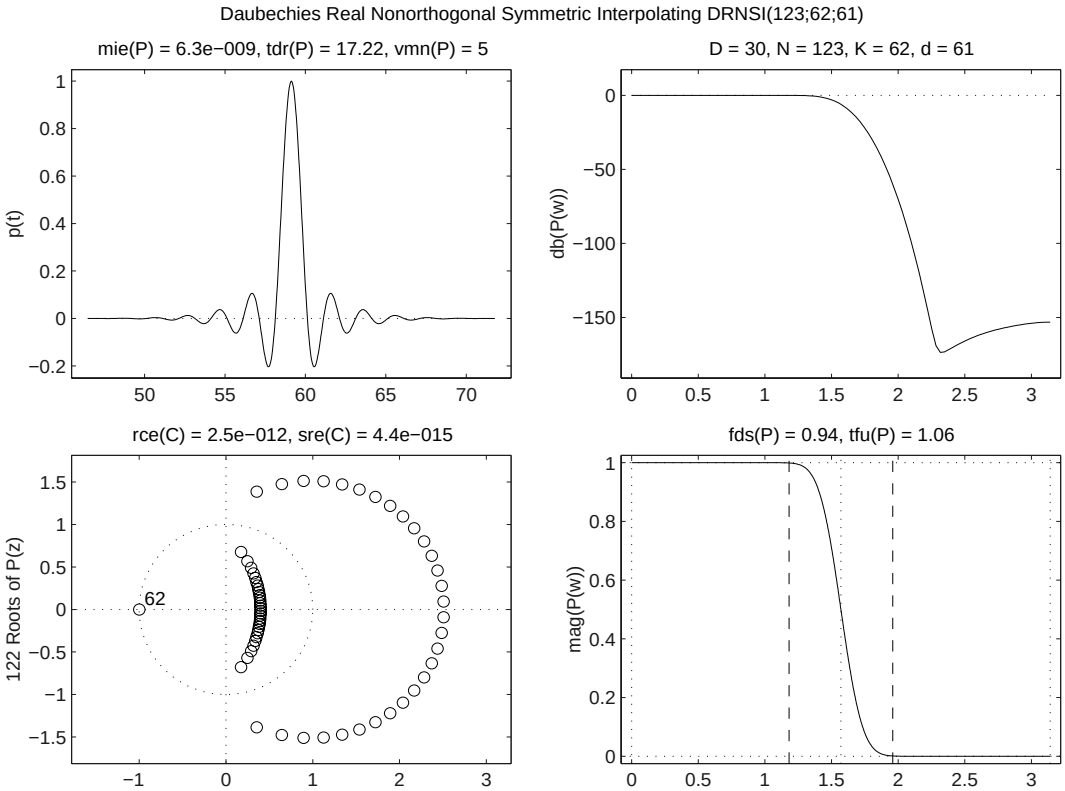

Figure 2: DRNSI(123;62;61) Filter Roots, Impulse Response, Frequency Response.

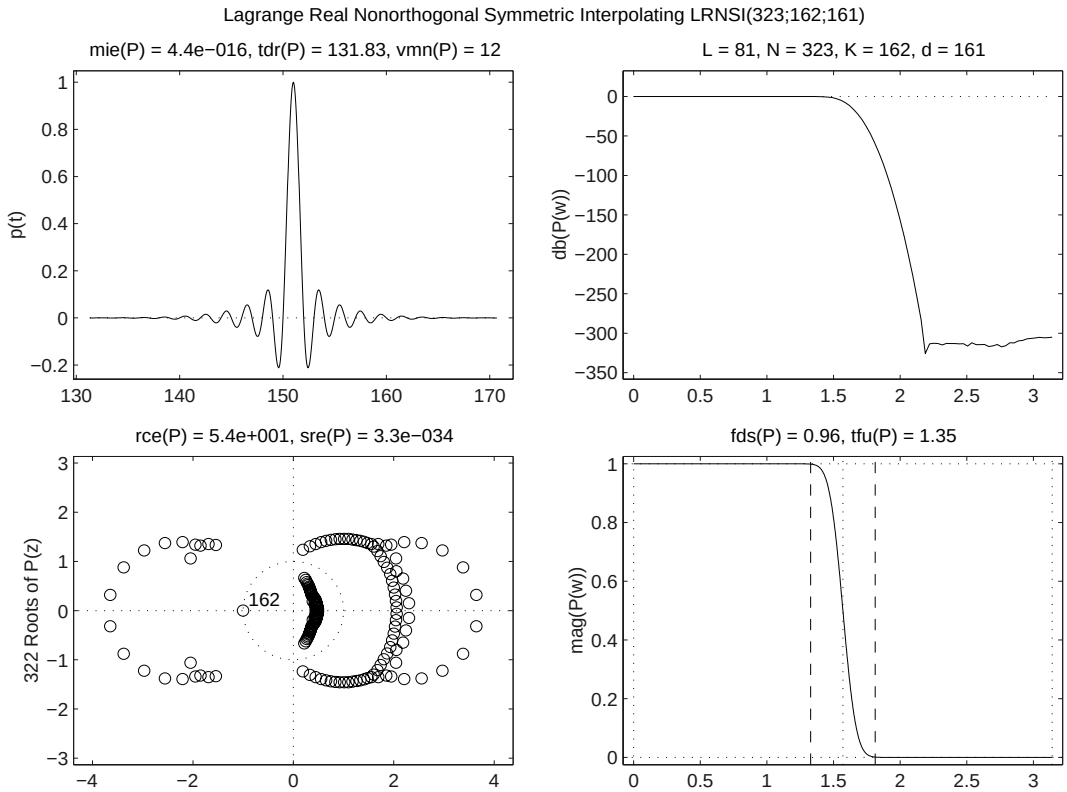

Figure 3: LRNSI(323;162;161) Filter Roots, Impulse Response, Frequency Response.

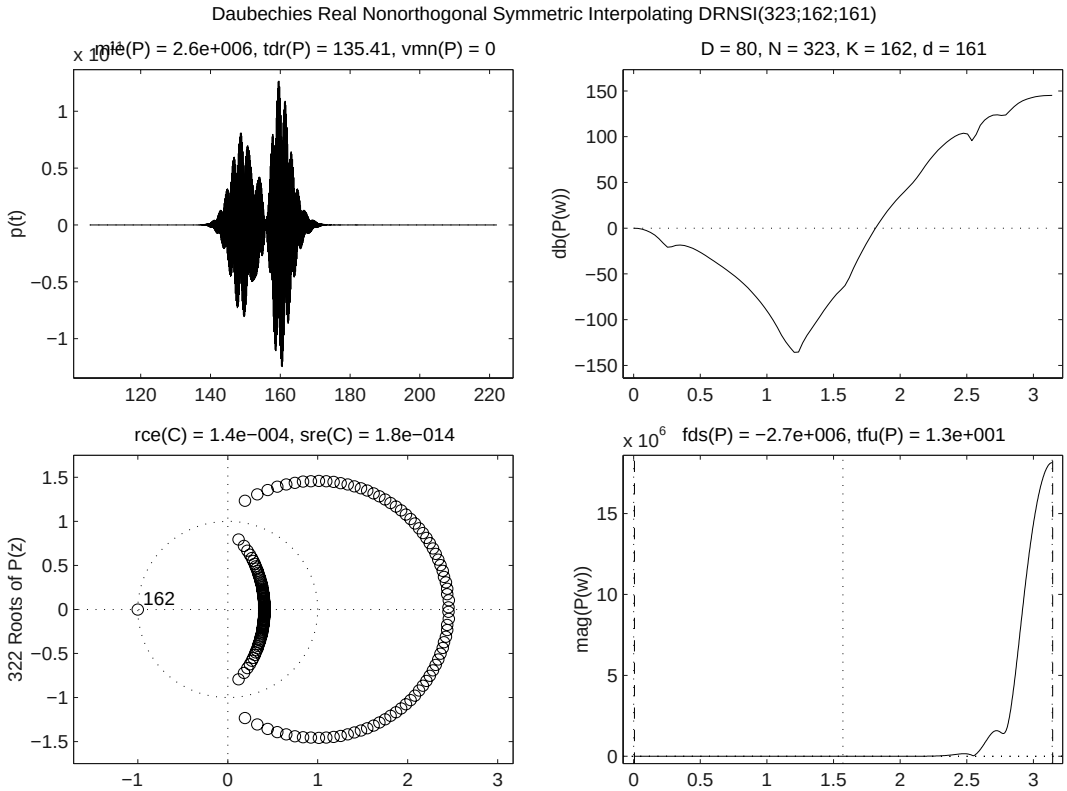

Figure 4: DRNSI(323;162;161) Filter Roots, Impulse Response, Frequency Response.

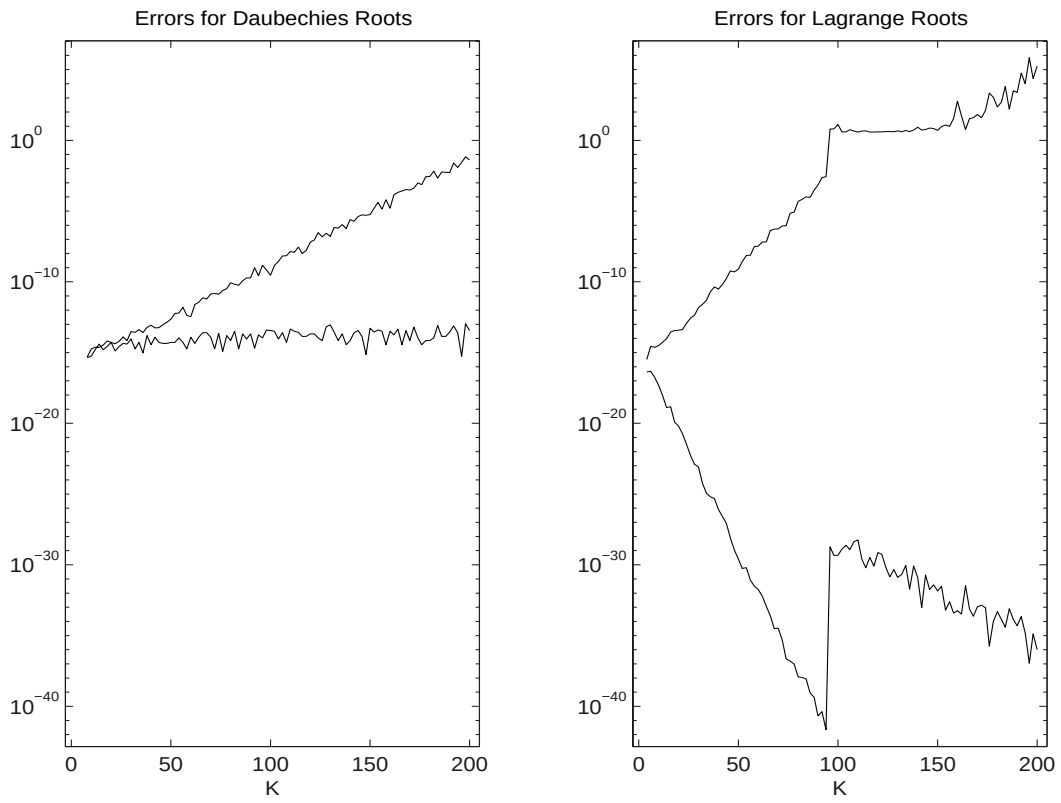

Figure 5: Lagrange and Daubechies Polynomial Root Errors.

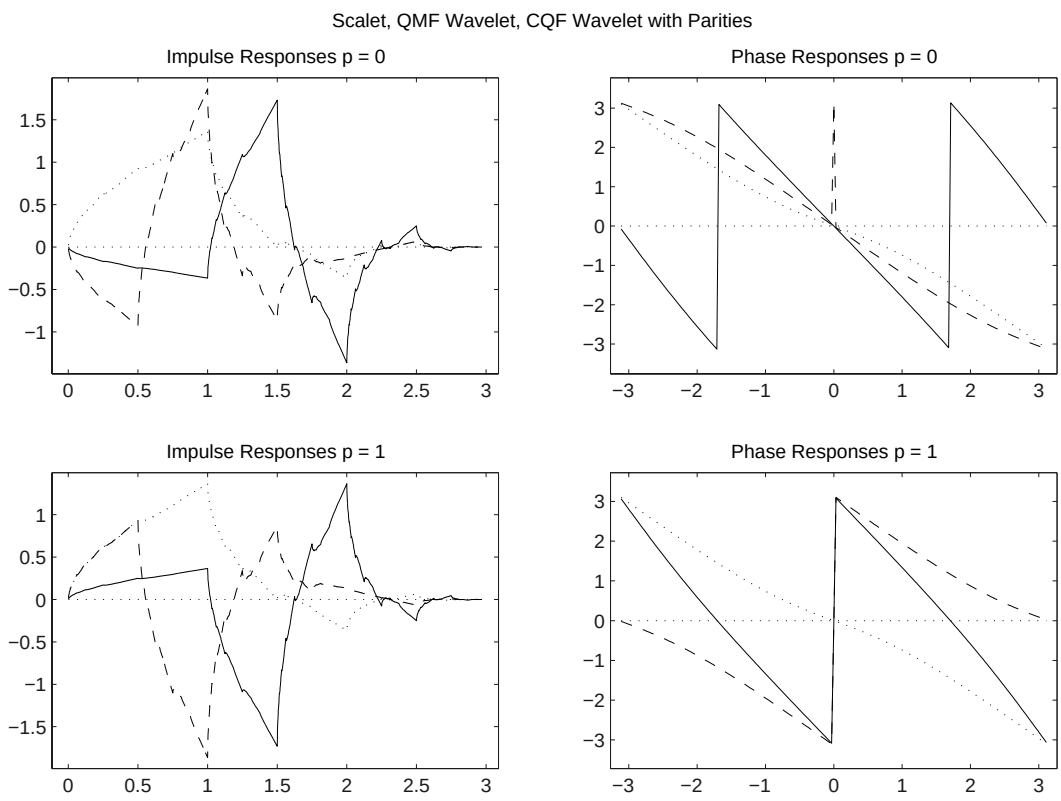

Figure 6: DROMD(4;2) Scalet, QMF, CQF Wavelets with Alternate Parities.

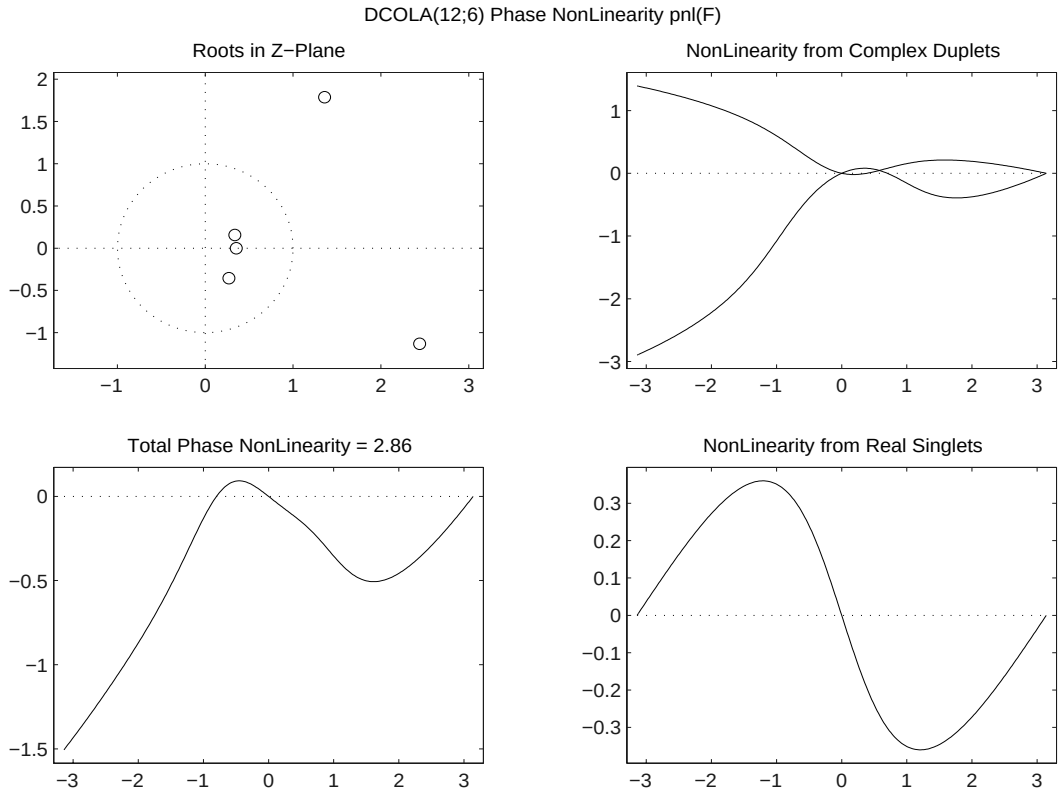

Figure 7: DCOLA(12;6) Phase NonLinearity.

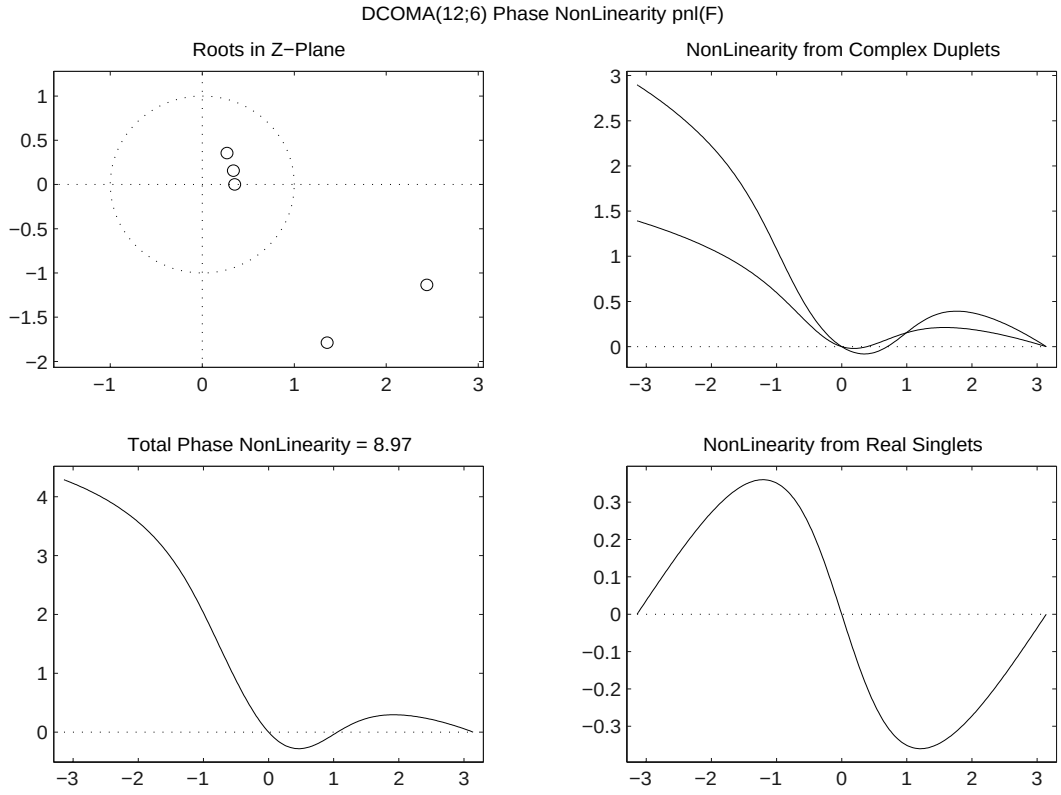

Figure 8: DCOMA(12;6) Phase NonLinearity.

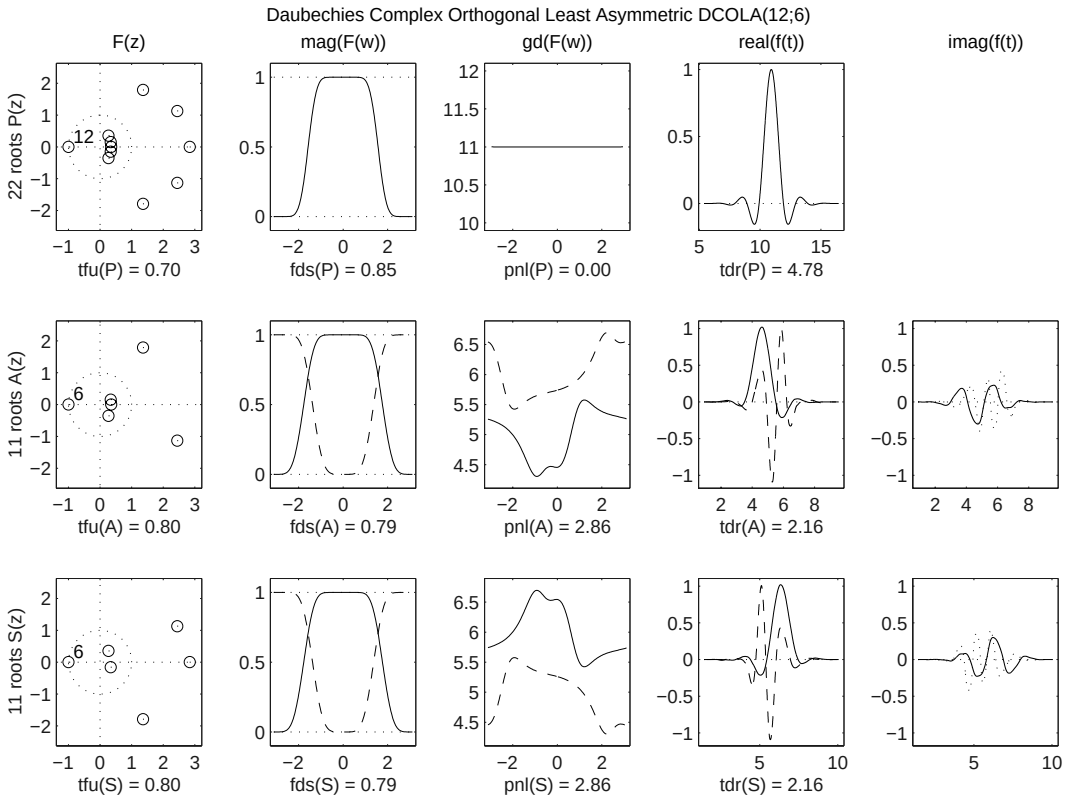

Figure 9: DCOLA(12;6) Spectral Factorization.

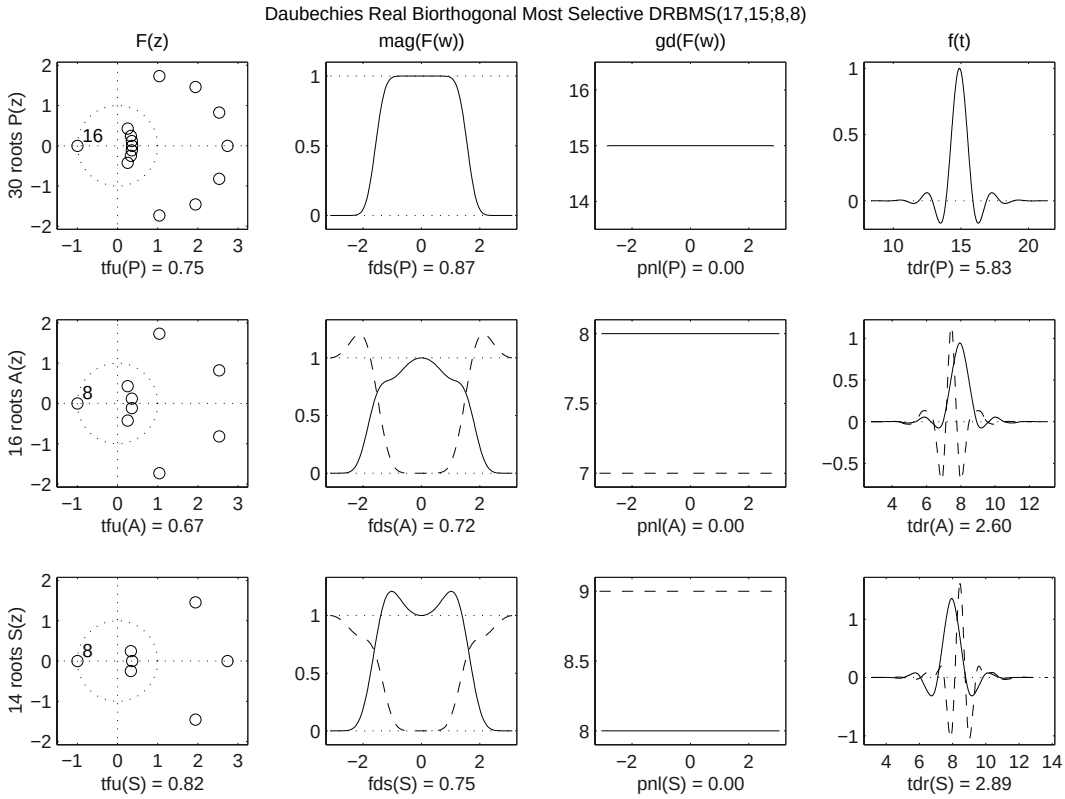

Figure 10: DRBMS(17,15;8,8) Spectral Factorization.

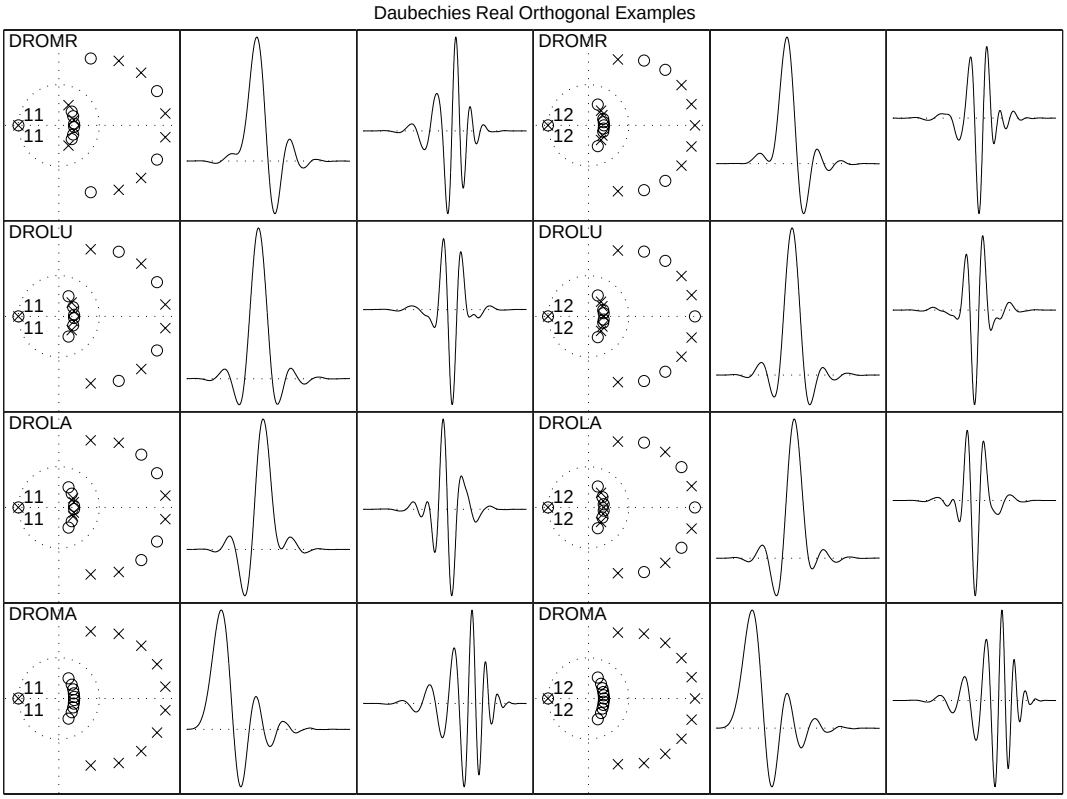

Figure 11: Daubechies Real Orthogonal Examples.

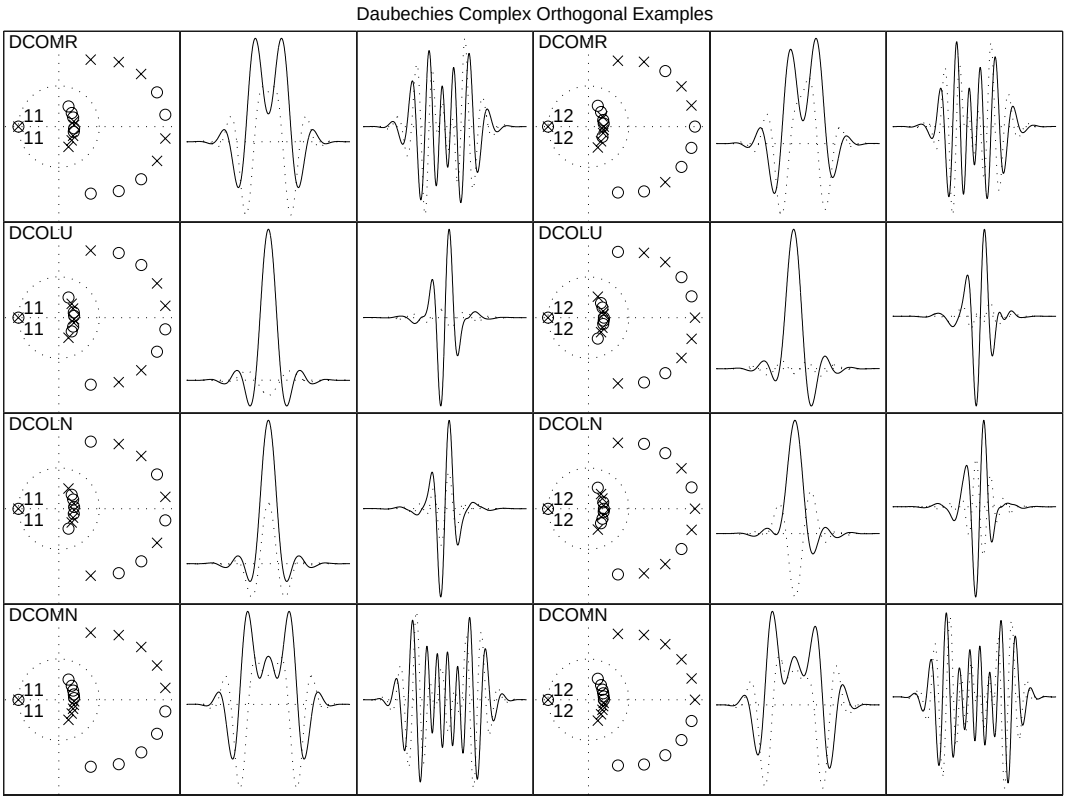

Figure 12: Daubechies Complex Orthogonal Examples.

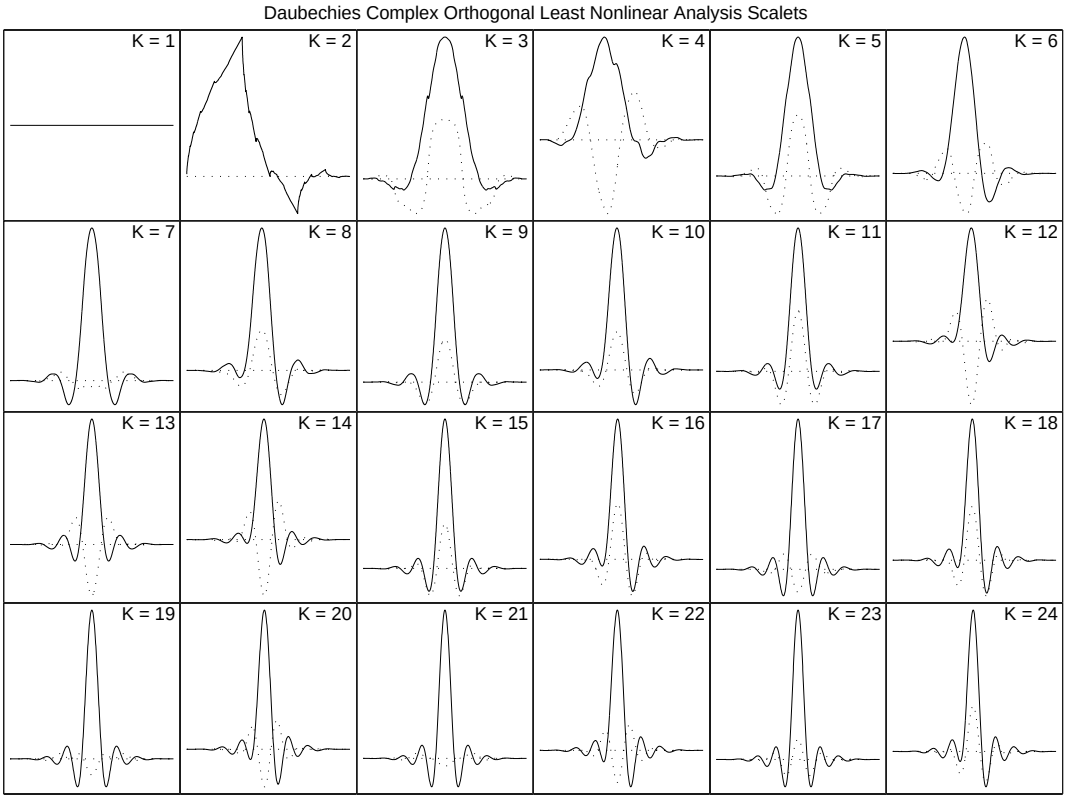

Figure 13: DCOLN Analysis Scalets.

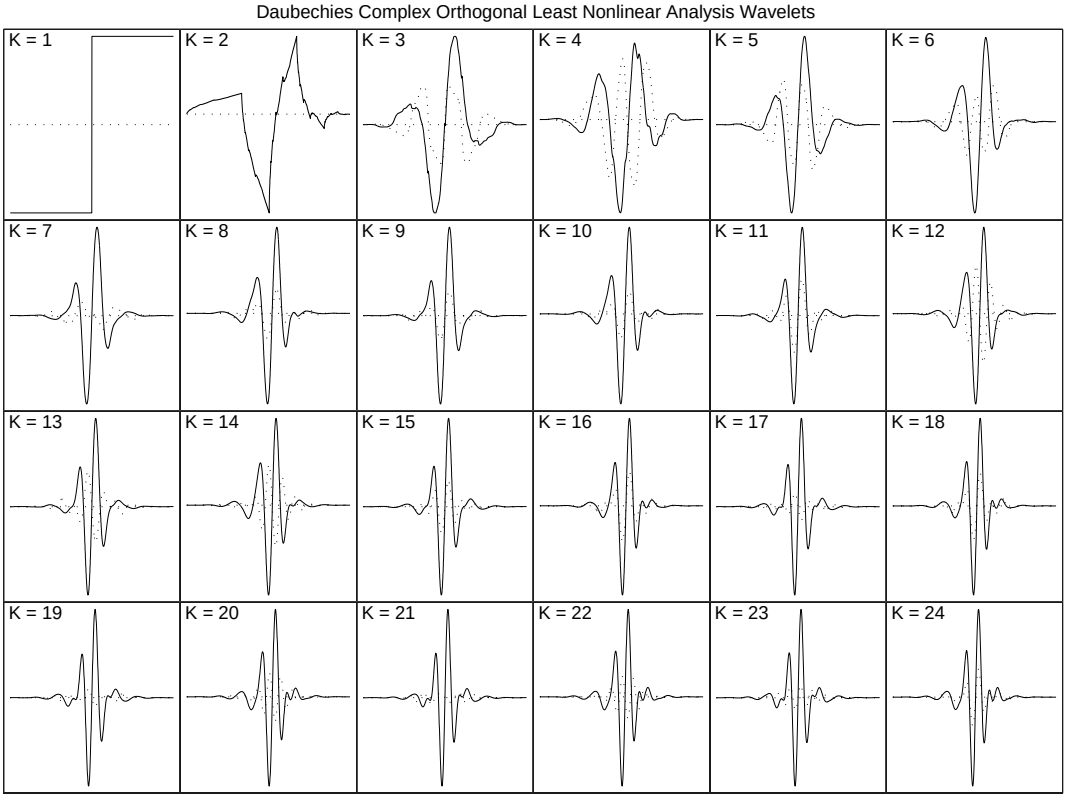

Figure 14: DCOLN Analysis Wavelets.

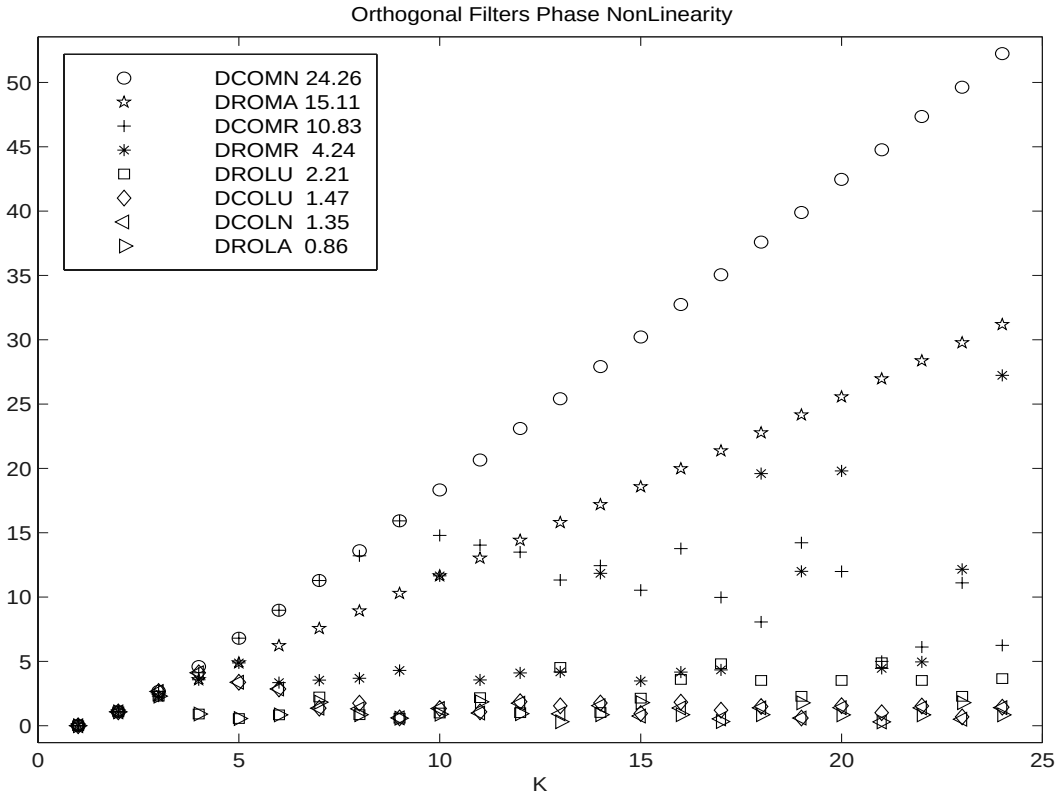

Figure 15: Phase NonLinearity of Orthogonal Filters.

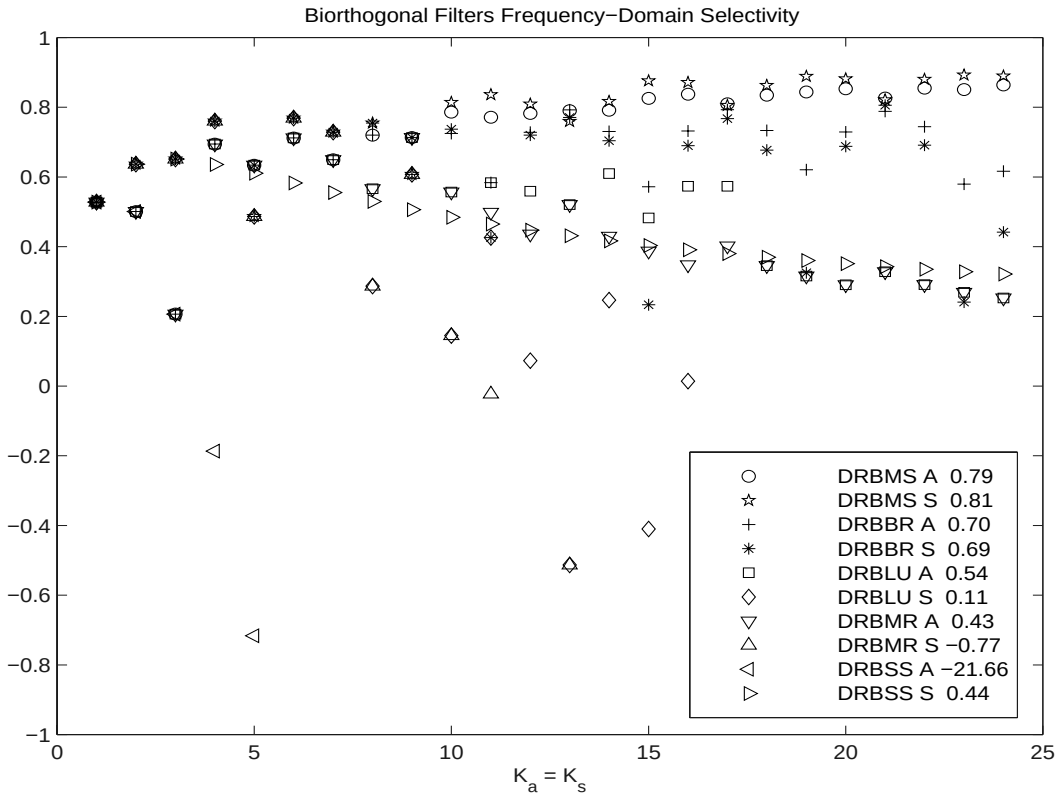

Figure 16: Frequency-Domain Selectivity of Biorthogonal Filters.